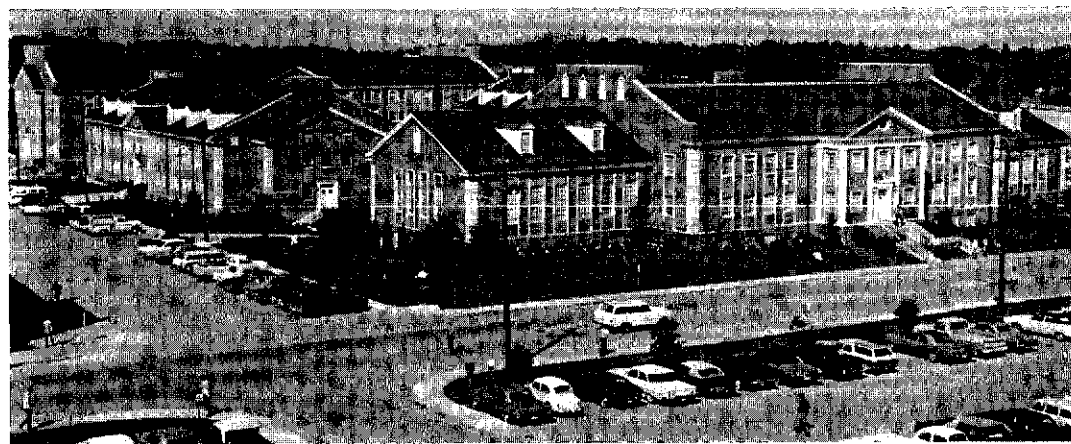


24P

COLLEGE OF ENGINEERING



Engineering Complex

(NASA-CR-138617)	OVONIC SWITCHING IN TIN	N74-27259
SELENIDE THIN FILMS	Ph.D. Thesis	
(Tennessee Technological Univ.)	113 p HC	
\$8.75	CSCI 20L	Unclas
		G3/26 41192

TENNESSEE TECHNOLOGICAL UNIVERSITY
COOKEVILLE, TENNESSEE

AN ABSTRACT OF A DISSERTATION

OVONIC SWITCHING IN TIN SELENIDE THIN FILMS

Charles Ronald Baxter

Doctor of Philosophy--Engineering

Amorphous tin selenide thin films which possess Ovonic switching properties are fabricated using vacuum deposition techniques. Results obtained indicate that memory type Ovonic switching does occur in these films with the energy density required for switching from a high impedance to a low impedance state being dependent on the spacing between the electrodes of the device. There is also a strong implication that the switching is a function of the magnitude of the applied voltage pulse. A completely automated computer controlled testing procedure is developed which allows precise control over the shape of the applied voltage switching pulse. A survey of previous experimental and theoretical work in the area of Ovonic switching is also presented.

OVONIC SWITCHING IN TIN SELENIDE THIN FILMS

A Dissertation

Presented to

the Faculty of the Graduate School
Tennessee Technological University

In Partial Fulfillment
of the Requirements for the Degree
Doctor of Philosophy
Engineering

by

Charles Ronald Baxter

June 1974

TABLE OF CONTENTS

	Page
LIST OF TABLES	vi
LIST OF FIGURES	vii
LIST OF SYMBOLS	x
Chapter	
1. INTRODUCTION	1
2. AMORPHOUS SEMICONDUCTOR SWITCHING	6
FABRICATION	7
CHARACTERISTICS OF OPERATION	8
Current Voltage Characteristics	8
Switching Parameters	11
SWITCHING MECHANISMS	18
SUMMARY	25
3. AMORPHOUS SEMICONDUCTOR MODELS	27
ORDER-DISORDER IN AMORPHOUS MATERIALS	29
THEORETICAL MODELS	30
Basic Electronic Structure	31
Basic Band Model (BBM)	36
Cohen, Fritzsche and Ovshinsky Model (CFO)	38
Henisch, Fagen, and Ovshinsky Model (HFO)	43
SUMMARY	43

Chapter	Page
4. EXPERIMENTAL PROCEDURE	48
FILM FABRICATION	48
FILM TEST PROCEDURES	59
ANALYSIS PROCEDURE	69
5. RESULTS	73
6. SUMMARY, CONCLUSIONS AND PROPOSED FUTURE WORK	92
SUMMARY	92
CONCLUSIONS	96
PROPOSED FUTURE WORK	97
BIBLIOGRAPHY	100
APPENDIXES	103
A. Program to Control Testing Procedure	104
B. Program to Monitor Deposition Rate	108
C. Program to Plot Resistance Versus Time	111
D. Program to Plot Resistance Versus Energy Per Unit Volume	114
E. Program to Plot Percentage Decrease in Resistance Versus Energy Per Unit Volume	117
VITA	120

LIST OF TABLES

Table		Page
4.1.	Sample of Output Data Obtained During Sample Testing	63
4.2.	Samples Used for Comparison of Switching Characteristics	68
5.1.	Energy of Switching Pulses	74
5.2.	Results Obtained in Switching a Sample Between Two Stable Resistance States	90

LIST OF FIGURES

Figure	Page
1.1. Cross Section View of Thin Film Thermistor in Flight Configuration	3
1.2. Plot of Log of Resistance Versus Reciprocal Temperature for a Tin Selenide Sample with a .010" Gap (N-6-A-10)	4
2.1. Cross Section View of a Thin Film Ovonic Switch (Planar Type)	9
2.2. Cross Section View of a Thin Film Ovonic Switch (Sandwich Type)	10
2.3. Typical I-V Characteristics of an Ovonic Threshold or Memory Switch	12
2.4. Plot of Energy Versus Time for Pulses Used in Setting and Resetting Processes	14
2.5. Plot of Threshold Voltage Versus Electrode Separation (Film Thickness) for $\text{Te}_{81}\text{Ge}_{15}\text{Sb}_2\text{S}_2$ [10]	16
2.6. Plot of Threshold Voltage Versus Temperature for a Threshold and Memory Device. The memory device was set after each measurement [10]	17
3.1. Energy Band Diagram of a Pure Semiconductor at 0°K	32
3.2. Plot of Density of States Versus Energy for an Intrinsic Semiconductor	35
3.3. Plot of Density of States Versus Energy for an Amorphous Semiconductor	37
3.4. Variation of Density of States of an Amorphous Semiconductor Due to Defects Such as Vacancies, Voids, and Impurities	39

Figure	Page
3.5. Variation of Density of States for Alloys Having Both Compositional and Positional Disorder	40
3.6. The Cohen, Fritzsche, Ovshinsky Model for the Density of States of a Typical Chalcogenide Glass	42
3.7. The Thermal Model of Threshold Switching	46
4.1. Cross Section View of Typical Ag-SnSe Devices	49
4.2. Vacuum Evaporation System for Deposition of Materials	50
4.3. Calibration Curves for the Deposition of Ag and SnSe	52
4.4. Mask Patterns Through Which Initial Films Were Evaporated	53
4.5. Mask Patterns Used in Fabricating Final Devices	54
4.6. Block Diagram of Data Acquisition System	56
4.7. Variations in Deposition Rate Typical of Materials Obtained from Source A	57
4.8. Variations in Deposition Rate Typical of Materials Obtained from Source B	58
4.9. Schematic Diagram of Linear Amplifier Circuit	61
4.10. A Sample Plot of Data Obtained During a Test Cycle	65
4.11. Plot of Amplifier Voltage Versus D/A Voltage with the Load Resistance as a Parameter	72
5.1. Switching Characteristics of Sample A3	75
5.2. Switching Characteristics of Sample C1	76
5.3. Switching Characteristics of Sample C2	77
5.4. Switching Characteristics of Sample C3	78

Figure	Page
5.5. Switching Characteristics of Sample D3	79
5.6. Switching Characteristics of Sample E1	80
5.7. Switching Characteristics of Sample E2	81
5.8. Switching Characteristics of Sample E3	82
5.9. Switching Characteristics of Sample F2	83
5.10. Switching Characteristics of Sample F3	84
5.11. Switching Characteristics of Sample G3	85
5.12. Switching Characteristics of Sample H2	86
5.13. Plot of Gap Width Versus Energy/Volume Showing the Range in Which Switching Occurred	89

LIST OF SYMBOLS

Symbol	
$\overset{\circ}{A}$	Angstrom units ($10^{-10}m$)
D	Pulse width (seconds)
E	Energy (joules) or (electron volts)
E_c	Energy at the bottom of the conduction band (electrons volts)
E_f	Fermi energy (electron volts)
E_g	Energy gap (electron volts)
E_v	Energy at the top of the valence band (electron volts)
E_s	Energy (joules)
F	Decay time (seconds)
I_H	Holding current (amps)
L	Gap length (meters) or (mils)
R	Resistance (ohms)
S_F	Percentage decrease in resistance
T	Film thickness (meters)
V	Pulse height (volts)
V_A	Output voltage of amplifier (volts)
$V_{D/A}$	Output voltage of digital to analog converter
V_H	Holding voltage (volts)
V_T	Threshold voltage (volts)
V_s	Volume (m^3)
W	Gap width (meters) or (mils)

Symbol

t_d	Delay time (seconds)
t_R	Recovery time (seconds)
t_s	Switching time (seconds)
μ	Micron (10^{-6}m)
ρ	Resistivity (ohm-cm)
σ	Electrical conductivity (mhos/m)

CHAPTER 1

INTRODUCTION

The National Aeronautics and Space Administration conducts worldwide meteorological rocket soundings to obtain measurements of the properties of the upper atmosphere such as temperature, pressure, density, and motion. The purpose of that project is twofold: first, to lead to better short and long range weather forecasting and, second, to supply data needed for missile and space vehicle launches. The measurements are made by using a sounding rocket to carry an instrument package to a desired altitude. At peak altitude, the rocket nose cone which contains the instrumentation package is ejected and the measurements are telemetered to the ground as the payload descends on a parachute.

The payload includes a temperature sensor used to measure atmospheric temperature during the descent. A bead type thermistor is presently being used to measure temperature and it gives accurate results up to approximately 55 kilometers (34.2 miles). Studies have shown that a thin-film thermistor should have the sensitivity necessary to extend the peak altitude from 55 kilometers to about 80 kilometers. [1]

The Department of Electrical Engineering at Tennessee Technological University was awarded a NASA research grant in

an effort to obtain a thin-film sensor which had the necessary temperature dependence as well as long term stability. Investigations by Ooten [1], Bynum [2], and Palmer [3] have led to the present device flight configuration shown in cross section in Fig. 1.1. Bynum [2] investigated the effects of silver migration on the study of a thin-film tin selenide thermistor and observed inconsistent resistance-temperature characteristics of the type shown in Fig. 1.2.

These fluctuations were assumed to be the result of passing too much current through the device during test procedures and Ovonic switching was suggested as a possible cause of the observed inconsistencies. Ovonic switching is a change that occurs in the conductivity of an amorphous semiconductor following the application of a voltage pulse. This phenomena will be discussed in detail in subsequent chapters.

Since tin selenide is the amorphous semiconducting material being used as the sensor in the thin-film devices being studied for NASA, an investigation of the electrical switching properties of the material was necessary in order to determine under what conditions fluctuations in resistance would be encountered. Because switching is a detrimental factor in obtaining stable resistance-temperature characteristics, a knowledge of what voltage levels cause switching to occur is essential.

This dissertation will be concerned with trying to isolate the conditions under which tin selenide films switch.

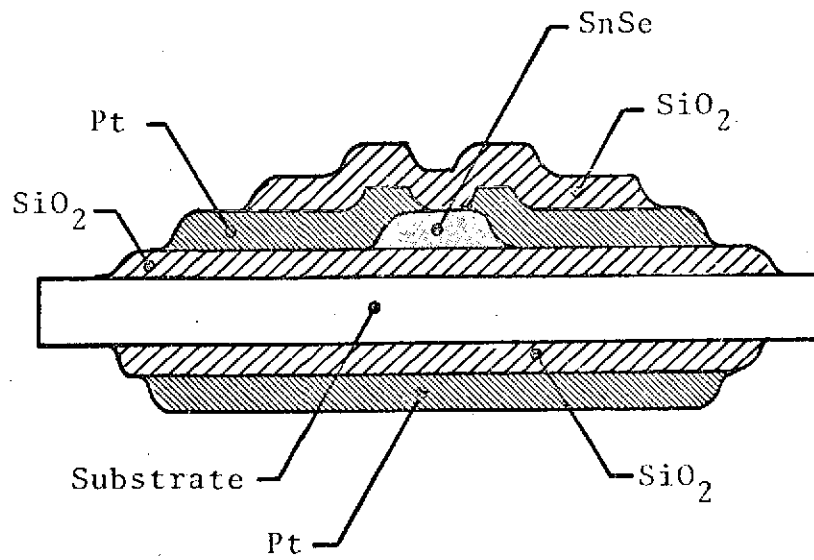


Figure 1.1. Cross Section View of Thin Film Thermistors in Flight Configuration

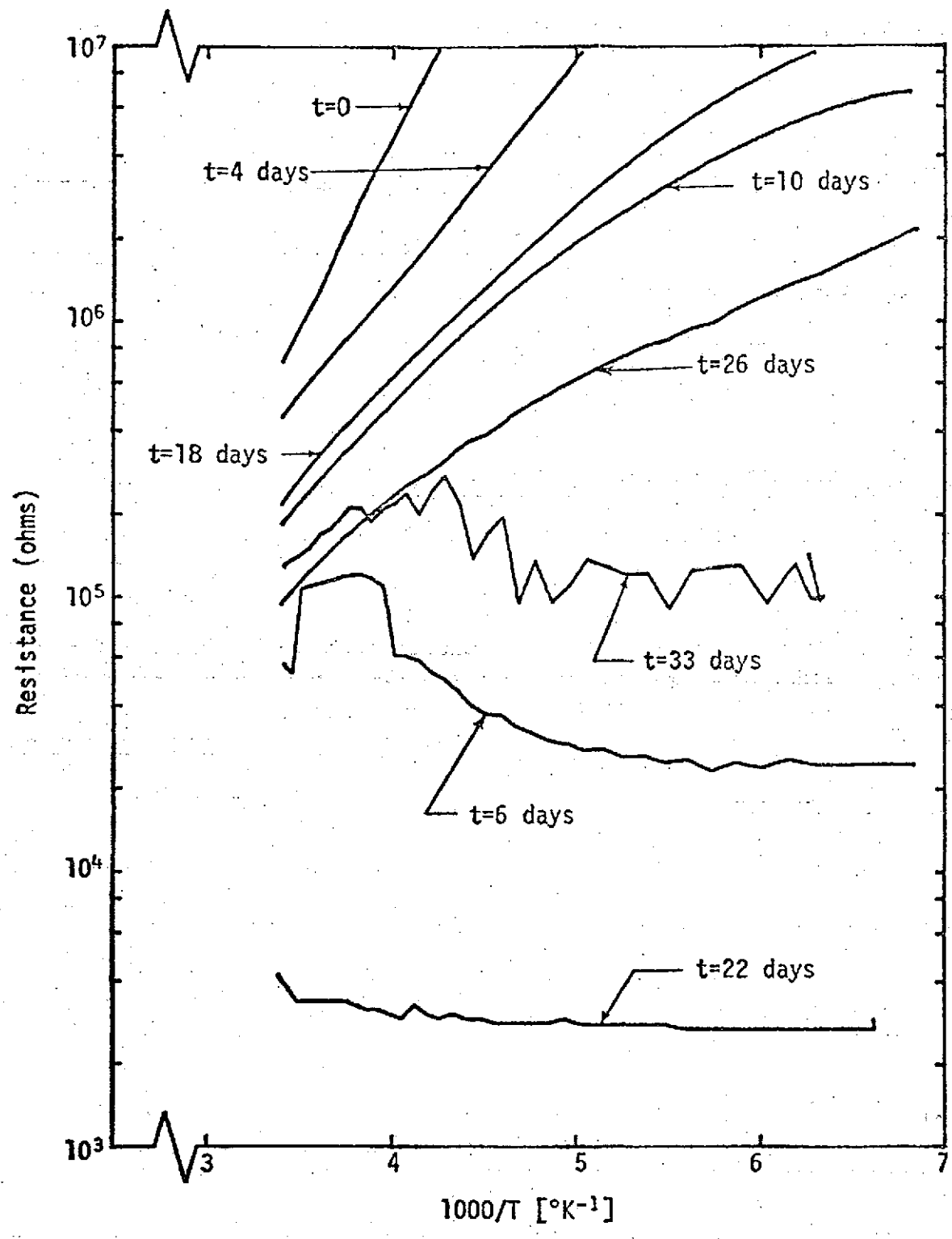


Figure 1.2. Plot of Log of Resistance Versus Reciprocal Temperature for a Tin Selenide Sample with a .010" Gap (N-6-A-10)

In particular, it is important to determine whether the switching is erratic or if the device has more than one stable state. By isolating the switching conditions, it should be possible to fabricate sensors which do not exhibit switching characteristics.

CHAPTER 2

AMORPHOUS SEMICONDUCTOR SWITCHING

In recent years semiconductor devices of a novel kind have been made from materials that are neither crystalline nor highly pure. These substances are in fact amorphous; that is, they have a disordered atomic structure. Amorphous devices are presently being studied in laboratories around the world and lend themselves to many novel applications. The most important examples of such devices are the threshold and memory devices which have been named Ovonic switches by their inventor Stanford R. Ovshinsky, who pioneered the work in this area beginning in 1958.

The metastable structure of these amorphous semiconductors gives them certain unique properties that are of considerable technological significance. One property is that they are structurally disordered and, therefore, relatively insensitive to high energy radiation and bombardment [4]. In the area of electronic switching, the amorphous material is changed from a disordered or glassy state to a more ordered structure. The transformations involved in this process have a marked influence on the electrical, optical, chemical, and mechanical properties of the amorphous materials, with these properties being dependent on film preparation.

FABRICATION

The properties of bulk Ovonic devices do not seem to depend critically on the fabrication method and, moreover, are insensitive to most trace impurities. However, the processes used in manufacturing these devices should be carefully optimized to insure devices with precisely repeatable characteristics and long operating life. The ultraclean concept associated with fabricating single crystal semiconductors does not appear to be a problem in this area.

Switching properties have been observed and studied in numerous amorphous materials. These materials include the elemental semiconductors germanium, silicon, tellurium, and sulfur; the covalent semiconductors such as GeTe, As_2Se_3 ; and the chalcogenide, arsenide, and boride glasses. Work has also been done on ionic amorphous semiconductors such as V_2O_5 , Al_2O_3 , and the transition-metal oxide glasses.

Glasses which are useful as amorphous semiconductors generally contain from two to four elements. From a switching standpoint, the most important group of glasses is probably the chalcogenides. Chalcogenide glasses contain at least one element from Group VIA of the periodic table: oxygen, sulfur, selenium, and tellurium. These glasses include binary, ternary, and quaternary systems. They can be cast, extruded, rolled, hot-pressed, blown, deposited by evaporation in a vacuum, or sputtered.

An important feature of Ovonic devices is that, unlike many other solid-state devices, they are uniquely adapted to thin-film circuitry. This could be a very important factor in large-scale integration. Thin-film ovonic switches can take various forms. [5] Two of these forms, the planar type and the sandwich type, are shown in Fig. 2.1 and Fig. 2.2.

Figure 2.1 represents one of the simplest thin-film ovonic structures in which an amorphous semiconductor material serves as a bridge between two electrodes. In the more elaborate configuration of Fig. 2.2, the active semiconductor material fills a position that is sandwiched between two electrodes. The electrodes in turn are overlain by contacts.

CHARACTERISTICS OF OPERATION

Current-Voltage Characteristics

The threshold and memory devices are closely related, but their physical mechanisms are quite different. Behavior with respect to time constants, voltages, and current levels leads one to believe that several mechanisms may be involved. More will be said about this effect later.

Both the threshold switch and the memory switch are normally in a high impedance state after fabrication. This state is called the nonconducting or "off" state. Both switches exhibit a threshold voltage V_T , above which the material exhibits a low impedance behavior. The transition from a high impedance to a low impedance represents a

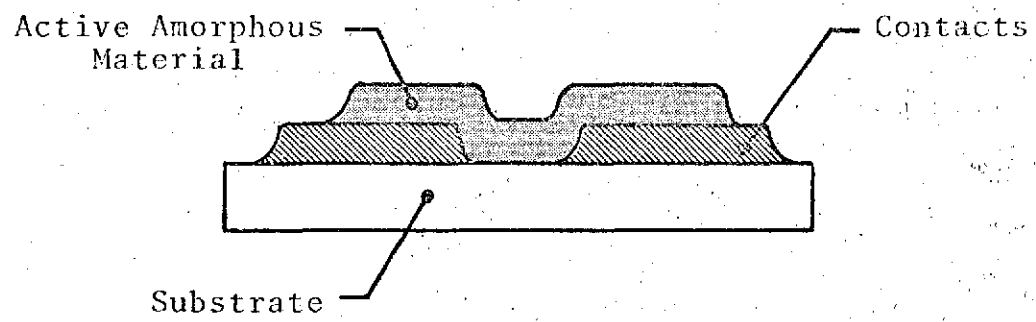


Figure 2.1. Cross Section View of a Thin Film Ovonic Switch (Planar Type)

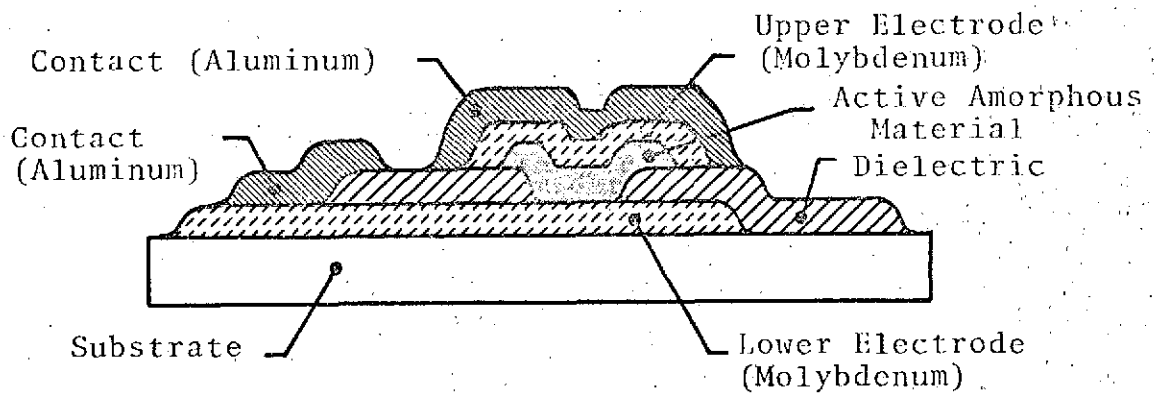


Figure 2.2. Cross Section View of a Thin Film Ovonic Switch (Sandwich Type) [5]

negative-resistance region on the I-V characteristic. The low impedance state is the conducting or "on" state of the switch. If the current through the threshold switch is quickly reduced below a critical value I_H called the holding current, the device will return to the "off" state; whereas, in the memory switch, if the device is kept in the "on" state for a critical time termed "lock-on," a further decrease in voltage is noted and the sample will remain highly conductive even if the applied voltage is completely removed. Once in the "on" state, the memory switch will remain in this state until a reset pulse with a sharp trailing edge is applied. This causes the memory switch to return to the nonconducting or high impedance state. A typical plot of the current-voltage characteristics of these devices is shown in Fig. 2.3.[6]

Switching Parameters

The major switching parameters are the threshold voltage V_T , the threshold current I_T , the delay time t_o , the switching time t_s , the holding voltage V_H , and the recovery time t_R . [6] These parameters not only depend on temperature, pressure, and composition, but also on the fabrication process, thermal and electronic history, and the nature of the electrodes. Because of this complex dependence, it is very difficult to compare results even on the same films. For this reason, it is more appropriate to discuss the results of previous work individually rather than collectively.

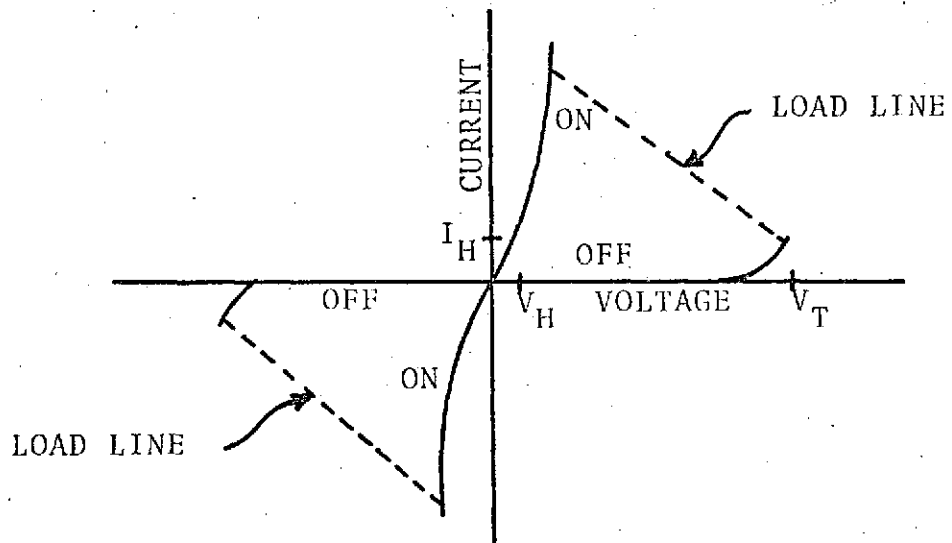


Figure 2.3. Typical I-V Characteristics of an Ovonic Threshold or Memory Switch

Neale, et.al., [7] discussed the switching process of a glass, the composition of which was not given. A 50 microjoule pulse applied in about 10 milliseconds was sufficient to change the material from a disordered or glassy state to a more ordered structure. This resulted in a resistance drop of three to four orders of magnitude. The device was returned to its high resistance state by applying a reset pulse of approximately 5 microseconds duration. This represented the injection of approximately 5 microjoules of energy into the sample, which supplied sufficient heat to return the material to the amorphous state. The sample cooled quickly and the disordered state was maintained at room temperature. A typical sample had a threshold voltage of about 15 volts, was about 1.5 microns thick and 5 microns in diameter, and cooled to room temperature in about one microsecond. The composition of the material was found to have a dramatic effect on the lifetime of the device. It was also determined that the energy-time combinations used for the set and reset operations profoundly affected the life expectancy of the device. Certain regions on the energy versus time plot shown in Fig. 2.4 resulted in effective setting and resetting of the device being investigated. It was found that energy-time combinations that fell below the roughly defined triangular regions would not produce stable changes in the state of the device even after repeated switchings. A device set within the set area must be reset at a compatible energy in the reset area. In other words, if a device is set within the ellipse

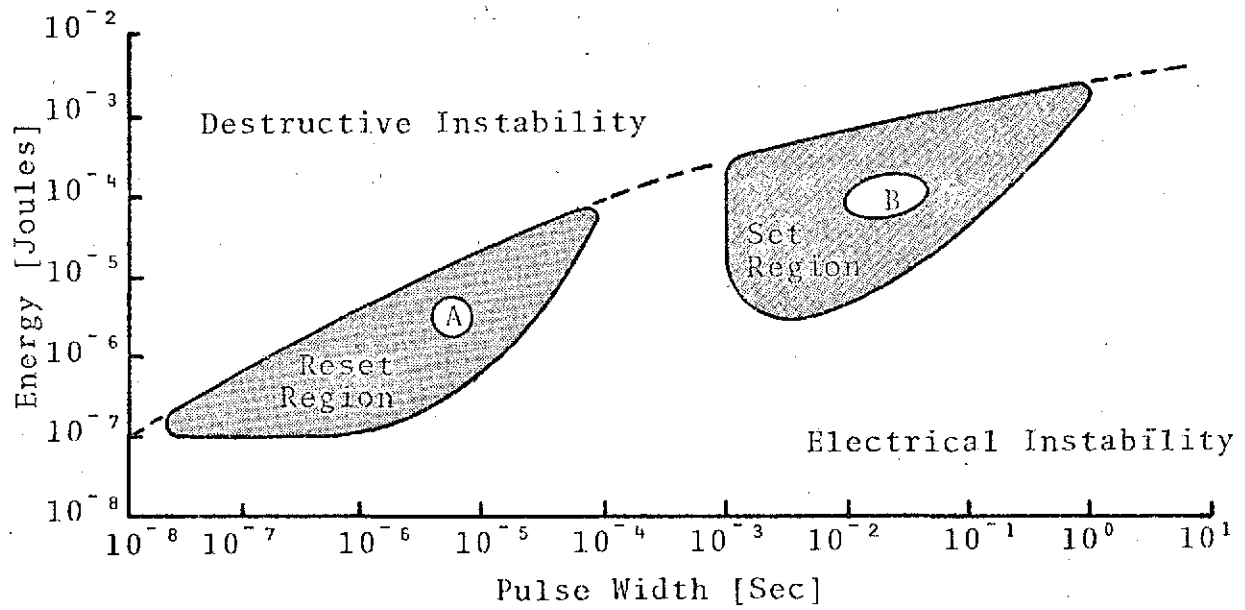


Figure 2.4. Plot of Energy Versus Time for Pulses Used in Setting and Resetting Processes [7]

marked B, then the proper reset condition would lie within the circle marked A. The reason for this correspondence is that the area of the converted or crystallized region in the amorphous semiconductor film depends on the set energy-time combination. As more material is converted to the ordered state, a larger energy is necessary to obtain a stable reversion.

For the sandwich type structure shown in Fig. 2.2, Ovshinsky and Fritzsche[8] and Adler and Moss[9] noted that the threshold voltage increases linearly with electrode separation. This result is shown in Fig. 2.5 for the memory material $\text{Te}_{81}\text{Ge}_{15}\text{Sb}_2\text{S}_2$. [8] The slope of the curve in Fig. 2.5 yields a threshold field of about 10^5 V/cm. The average threshold field is independent of thickness up to about 10μ and then decreases. The magnitude of V_T decreases with increasing temperature as shown in Fig. 2.6 for $\text{Te}_{40}\text{Ge}_7\text{As}_{35}\text{Si}_{18}$, which is a threshold material, and for $\text{Te}_{81}\text{Ge}_{15}\text{Sb}_2\text{S}_2$, which is a memory material.

As shown in Fig. 2.3, the conducting branch of the I-V characteristic is nearly vertical. That is, above the holding voltage V_H , the current is relatively independent of the applied potential. The value of V_H for a one micron thick chalcogenide film is typically one volt with electrodes of Mo, W, Ta, and nichrome, and 1.5 volts for carbon electrodes. The small voltage drop in the conducting state and the large resistance difference between the "off" and "on" states make these chalcogenide glasses suitable for switching and memory

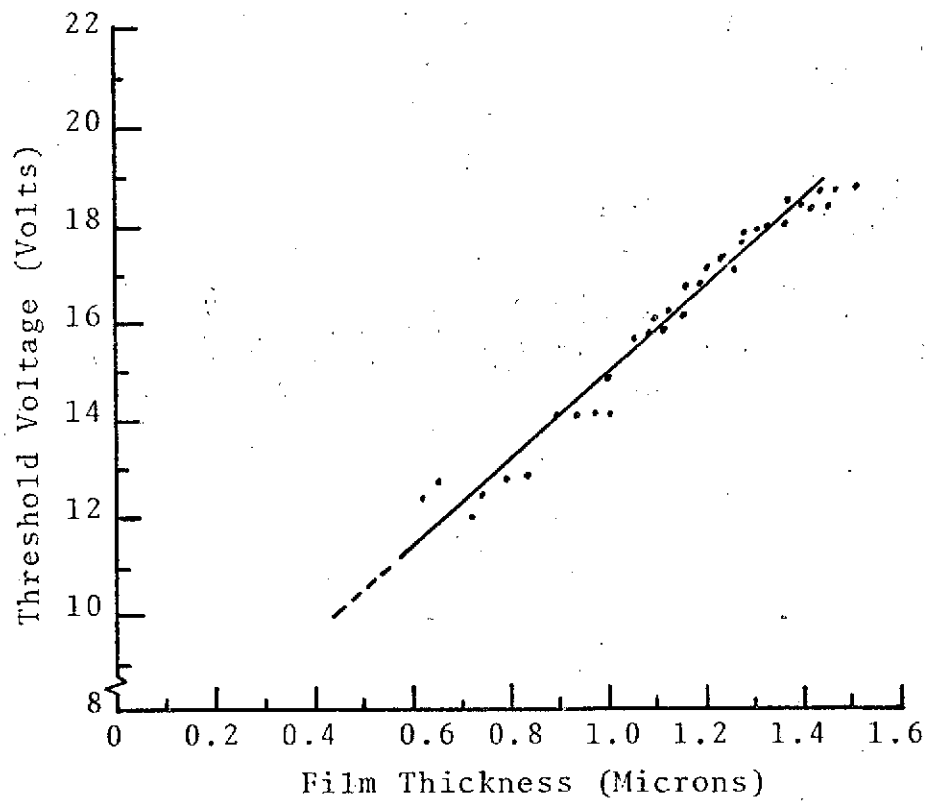


Figure 2.5. Plot of Threshold Voltage Versus Electrode Separation (Film Thickness) for $\text{Te}_{81}\text{Ge}_{15}\text{Sb}_2\text{S}_2$ [8]

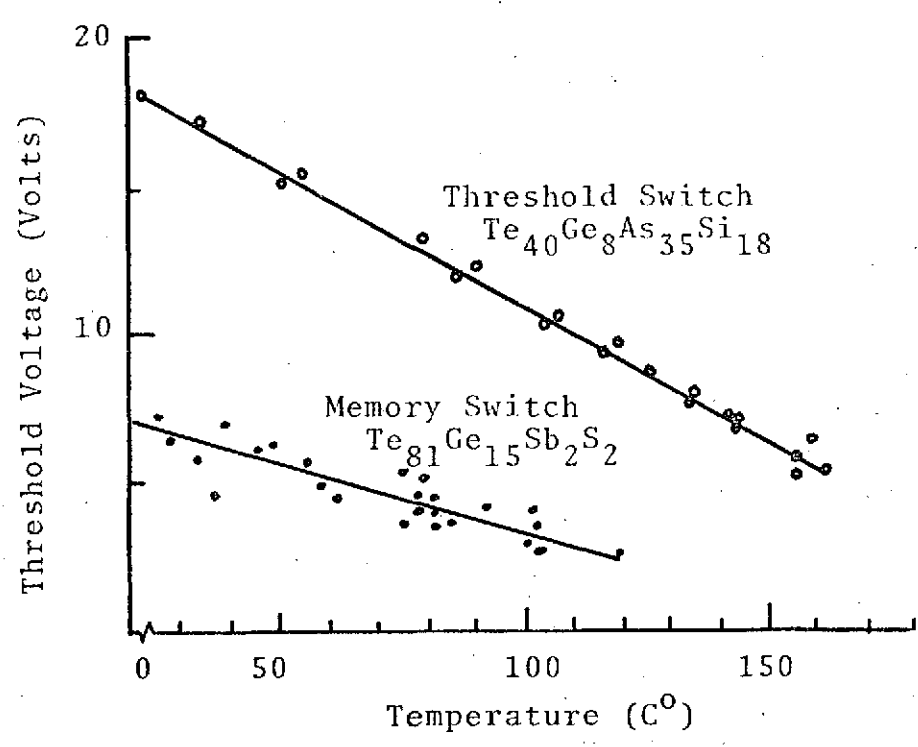


Figure 2.6. Plot of Threshold Voltage Versus Temperature for a Threshold and Memory Device. The memory device was set after each measurement [8].

applications. Ovshinsky and Fritzsche[8] observed that the holding voltage V_H was independent of temperature, electrode separation (for $0.4 < d < 5\mu$), electrode area, and current. They concluded that, since V_H is practically independent of electrode separation, the potential drop V_H occurs predominantly near the electrodes.

Adler[6] noted that a finite delay exists between the time that V_T is exceeded and the switching event. This delay time t_0 is of the order of several microseconds at threshold, but decreases sharply with increasing overvoltage, and reaches the order of nanoseconds if the voltage is fifty percent greater than V_T .

SWITCHING MECHANISMS

The mechanism of switching is as yet unresolved. There appears to be a lot of disagreement as to the actual cause of the switching process itself, with at least four models having been proposed. They are:

1. The switching is due to a heat-induced phase change that is propagated through the sample.
2. The amorphous medium undergoes a phase transformation when the valence electrons are liberated by the high electric field.
3. The switching is due to the formation of conducting filaments.
4. The switching is entirely thermal.

Since the switching mechanism is strongly influenced by the fabrication process and material composition, the results obtained by different authors using different compounds will be discussed individually, followed by a general summary.

Ovshinsky[10] has shown that one means of initiating switching in semiconducting glasses between two highly conductive electrodes can be caused by Joule heating of a current channel and results in a "pancake-shaped" temperature profile and thermally stabilized high-field effects close to the electrodes. He stated that the actual switching could not be thermal and that electronic processes involved prevented a thermal "runaway." A simple thermal "runaway" would require temperatures in the current channel far in excess of those that could be reached without destroying the sample.

Boer and Ovshinsky[11] have analyzed the switching mechanism in a semiconducting glass evaporated from an ingot of $\text{Ge}_{.12}\text{As}_{.3}\text{S}_{.25}\text{Se}_{.01}\text{Te}_{.22}\text{V}_{.1}$. Their analysis indicates that the actual switching involves electronic processes which prevent a thermal runaway. They concluded that, in Ovonic threshold switches of the type that were investigated, the switching transition is initiated by an electrothermal instability causing a high density current channel. A simple thermal runaway would require the current channel to have temperatures that would greatly exceed those that could be reached without material destruction.

Fritzsche and Ovshinsky[12] have stated that most materials cannot withstand electric fields larger than about

10^6 V/cm. For high resistance semiconductors, the breakdown frequently causes a regenerative structural change in the material or, without any material change, leads to a conducting state that is maintained only above a certain holding current. Both the mechanisms leading to breakdown and the processes that take place after breakdown are difficult to establish. These processes depend not only on electronic and conduction processes, but on the thermal and structural stability of the materials as well. Most nondestructive breakdown effects are current-controlled and a conductive state is reached with a simultaneous constriction of the flow to a path or channel whose cross section increases with the current.

Arguments against the possibility of explaining the switching observed in the Ovonic threshold switch and Ovonic memory switch by a thermal mechanism have been:

1. Apparent discontinuous change of slope from a positive differential resistance at the point of breakdown to that of the load line.
2. The observation, supported by pulse measurement, that during the delay time heating is rather insignificant.
3. The switching time of a fraction of a nanosecond, which is too short to permit heating of material in a sufficiently large current channel to a temperature which is high enough to achieve the conductance observed in the conductive state.

Guntersdorfer [13] has studied thermal effects connected with switching in commercial Ovshinsky switching elements consisting of two graphite pellets coated with a one micron Te-As-Ge-Si film and pressed tightly together in a

glass tube. He concluded that melting was unavoidably connected with switching in these devices and could not decide whether the switching process was initiated thermally or electronically.

Hensch and Pryor [14] have investigated Ovonic switching in encapsulated switches based on one micron films of $\text{Te}_{40}\text{As}_{35}\text{Ge}_7\text{Si}_{18}$ between graphite electrodes. They showed that the mechanism of threshold switching in thin chalcogenide glass systems is essentially nonthermal. They indicated that the problem of electronic versus thermal switching is in need of further study.

Weirauch [15] has investigated threshold switching and thermal filaments in amorphous semiconductors. A switching device 2mm by 3.6mm was fabricated by compressing a heated fragment of the nonoxide glass, $\text{As}_{20}\text{Ge}_{30}\text{Se}_{50}$, between carbon electrodes in a pyrex tube. Upon heating the device to 275°C and applying a sufficiently large AC voltage across the sample and 10 kilohm series resistor, threshold switching was observed. The device was placed in a tubular furnace with a viewing port. At the instant that switching occurred and with the aid of an infrared viewer, a bright filament was noted to extend between the two electrodes.

Baryshev [16] and others studied switching phenomena on the surface of glassy CdGeAs_2 . The device used was a diode structure formed by two tungsten point contacts on the surface of glassy CdGeAs_2 . The appearance of a filament in the form of a molten glass channel between electrodes was observed

when the device switched to the high conductivity state. The width of the filament ranged up to 1.8 microns. Upon applying a current pulse that destroyed the filament and increasing the voltage to the switching threshold, the new and old filaments between the electrodes did not coincide. These results were used to explain electrode burn out in thin film switches and instabilities in switching voltage.

Ovshinsky [10] has also described a rapid and reversible transition between a highly resistive and a conductive state which was observed in various types of disordered materials. The materials studied were oxide- and boron-based glasses and also materials that contained tellurium and/or arsenic combined with other elements from Groups III, IV, and VI of the periodic table.

Measurements were made on an amorphous semiconducting film of $\text{Te}_{48}\text{As}_{30}\text{Si}_{12}\text{Ge}_{10}$. The sample was 5×10^{-5} cm thick between carbon electrodes with a contact area of approximately 10^{-4} cm². The material had a room temperature resistivity of $\rho = 2 \times 10^7$ ohm-cm. A 60-Hz AC voltage was applied across the sample and a 10^4 ohm load resistor was used. The same switching characteristics were found to exist for both sputtered and hot-pressed samples even when the electrodes were of different contact areas or were of different materials. The threshold voltage V_T was found to increase linearly with film thickness even when different electrode materials were used. Threshold voltages between 2.5 and 300 volts were observed.

Upon switching to the low resistance state, a current filament appeared to form, growing in diameter with increasing current flow. Filament diameters of 5×10^{-3} cm were observed. Boer and coworkers have also observed similar filaments. By applying a rectangular voltage pulse across the sample, switching was found to occur after a delay time t_d with the duration of the switching process lasting less than 50 nanoseconds.

Stocker [17] has discussed switching and memory effects in thin film semiconducting chalcogenide glasses. Numerous thin film devices were fabricated by both thermal and flash evaporation. Different geometrical configurations, substrate materials, and contacting procedures were also used, but none of these things were found to have a marked effect on the electrical characteristics that were observed. The I-V characteristics of the thin film devices were found to be similar to those observed in bulk samples of the same material. A series of films of the same material but with varying thicknesses was prepared, but no significant correlation between film thickness and threshold voltage was found. The voltage required for the initial switching event was found to be normally higher than the threshold voltage observed under continuous AC operation. This initial voltage was found to be thickness dependent, similar to the dependence of the path forming voltage on the distance of the electrodes. Each of the devices was examined before and after the threshold switching. Evidence of partial

devitrification was found under the contact area in all cases. An Au-glass-Au thin film sandwich was evaporated onto a glass substrate. When an AC voltage of sufficient magnitude was applied across the sample to cause threshold switching, localized regions of devitrification could be observed. The word devitrification in this case implies a change in the physical structure of the glass film. The following qualitative model was proposed as an explanation for fast threshold switching:

1. Upon application of an electric field heating produces local devitrification. This process proceeds extremely rapidly and produces a filamentary path of devitrified material.

2. The current increases further until a limit determined either by the external circuit or the resistance of the structure is reached. The filamentary path now consists of molten material at high temperature.

3. Upon reducing the current, cooling results in the transformation of the molten filament into the glass state. The cooling rate must be fast enough so that transformation to the glassy state rather than phase separation occurs.

Although thermal switching is possible, it is probably not the sole cause of switching in Ovonic devices, as it would involve too much heating in too short a time. For thicker films there appears to be considerable evidence that the switching mechanism is thermal. For thin films under about 8 microns in thickness, the situation is not as clear, and one study suggested that the switching mechanism may be thickness dependent. Another study showed that, even for thin films, many switching properties can be explained from a thermal standpoint. Many investigators concluded that the

memory effect must be understood as a thermally induced crystallization of the amorphous material which leads to high conductivity. Several authors attributed switching to a filamentary plasma with high conductivity that travelled from one electrode to the other. Observations of melting and crystallization during switching and the dependence of switching characteristics on device thickness and temperature tend to support the thermal mechanism of switching.

SUMMARY

The application of amorphous semiconductor devices has increased in recent years. Chalcogenide glasses have received considerable attention because of their established or possible importance in the areas of electroplating, electrophotography, infrared transmitting windows, electronic switching, and electronic and optical memory applications. Threshold switches are being used in electroluminescent displays, AC thermostats, and logic circuits. Recent work on optical switching has helped to broaden the range of applications for memory switching. A recent development uses amorphous memory switching in a 256-bit electronically alterable read mostly memory [7] built by Energy Conversion Devices on substrates from Intel Corporation.

Because of the uncertainty which exists concerning the relative role of electronic and thermal switching mechanisms, it appears that much more experimental data is needed that can distinguish between them. One means of

gaining additional insight as to the switching mechanisms involved in thin film devices is to obtain more detailed data on the dependence of device behavior on thickness, temperature, deposition parameters, and composition. A study of the microscopic nature of the filaments observed during switching and their effects on electrical characteristics would help clarify some of the problems associated with memory devices.

One problem to be reckoned with is that of reproducibility. Reproducibility has long been a problem in this area. Sample reproduction is directly related to materials' characterizations, which in turn involves such things as chemical composition, whether or not the sample is truly and completely amorphous, and whether or not there are multiple phases present.

The field of amorphous semiconductor switching is a relatively new and exciting area. Whether or not these new devices can be fabricated into smaller, lower cost, more reliable devices and compete on the commercial market remains to be seen.

CHAPTER 3

AMORPHOUS SEMICONDUCTOR MODELS

Although there has been considerable interest in the last few years in the switching properties of amorphous semiconductors with an emphasis on the chalcogenide glasses, there is still no theory that adequately accounts for the observed characteristics [18]. Numerous mechanisms have been proposed to explain the observance of threshold switching in amorphous semiconductors. Adler [6] has stated that memory switching is simply an amorphous-crystalline transition which has now been confirmed in detail. He also stated that, except for the fact that memory switching was electrically induced and occurred after a prior threshold switching, the mechanism leading to memory switching was well understood and that the area of controversy was in the mechanisms leading to threshold switching. Owen and Robertson [19] have stated that threshold switching always precedes memory switching and that any mechanism established for the former is therefore applicable to the latter. Based on the observations of Warren and Adler, it seems that, qualitatively, memory switching is well understood from the standpoint of the amorphous-crystalline transformations involved, but quantitatively, there is not a rigid theory to support the observed characteristics of either the threshold or memory devices.

Considerable controversy exists as to whether threshold switching is primarily an electronic or a thermal process. Thermal mechanisms stress the importance of Joule heating in connection with the observed exponential increase in conductivity with temperature. When the rate of heating of a material rises rapidly and this heat cannot be conducted away, a very hot conducting filament appears to form between the electrodes of the device. However, Adler [6] claims that a pure thermal model cannot account for threshold switching in thin amorphous films since non-ohmic conduction has been shown to be due to an electronic mechanism. As a result, an electrothermal model of switching has been developed which appears to be in agreement with a variety of experimental data. The relative importance of these effects depends on the composition and thickness of the amorphous material, the nature of the contacts, and the device geometry. The controversy between thermal and electronic effects in regard to threshold switching is best summarized by Adler [6] when he states, "one particular device can exhibit either purely electronic or primarily thermal switching depending on the procedure used to induce the 'on' state."

Before discussing some of the theoretical models proposed to explain threshold switching in amorphous materials, the concept of order-disorder in amorphous solids should be mentioned.

ORDER-DISORDER IN AMORPHOUS MATERIALS

A perfect crystal in its ground energy state is said to have perfect compositional, positional, and magnetic (spin) order. This simply means that, if we know the position and type of any atom in the crystal and the crystal's orientation, we can determine the position and type of every other atom in the crystal. Crystals are never perfect, however, and we can classify their imperfections. The introduction of impurities into a crystal would result in compositional disorder, while defects that exist within the crystal are examples of positional disorder. There are also dynamic imperfections which can come into play. All amorphous solids have long-range positional disorder, but for the elemental amorphous semiconductors, this is the only type of disorder, while the amorphous compound semiconductors always possess both compositional and positional disorder.

The band theory of crystalline solids says that, for perfect periodicity of the atoms, the energy states that an electron can occupy as it moves in the solid are continuously distributed over energy ranges called bands, but are excluded from other energy ranges called gaps. It is interesting to note that the existence of periodicity is not essential in explaining the electrical properties of crystals. By taking materials through their melting point, which is the temperature at which long-range periodicity vanishes, it is found that, except for several materials whose short-range order changes discontinuously at the melting point and leads to a

semiconductor-metal transition, almost nothing happens to the electrical conductivity. This means that upon melting, metals remain metals, semiconductors remain semiconductors, and insulators remain insulators. Thus, one approach to take in determining the electrical properties of an amorphous material is to assume perfect short-range order and then introduce long-range disorder. This might include both a perturbation on the band structure and a scattering process that could limit the free carriers' mobility.

THEORETICAL MODELS

Because of the overabundance of models, both electronic and thermal, which have been proposed to explain the switching phenomena, it is impossible to discuss them all. The following discussion is a review of a few of the theoretical models proposed to describe the switching observed in amorphous semiconductors. The models presented below are electronic in nature, as they deal with conduction mechanisms that take place within the material as opposed to the thermal mechanisms which assume Joule heating as being the primary cause of switching. The following models were selected because they incorporate the basic ideas contained in other models. Electronic models seem to be at a disadvantage since the electronic structure in the amorphous state is not clearly understood and it is, therefore, difficult to discuss topics such as space-charge formation, non-ohmic behavior, and the roll of barriers at the electrodes, in anything other than

semiquantitative terms. Since a rigid theory in the area of amorphous semiconductors does not exist at this time and since a given set of data cannot be used to eliminate a particular model because different compositions and geometries lead to different switching mechanisms, each of the electronic models will be discussed individually, followed by a general summary.

Basic Electronic Structure

Before discussing the band structure of amorphous semiconductors, we need to briefly review the band structure of a typical intrinsic crystalline semiconductor. A crystalline semiconductor is one in which a band of electronic states, completely filled at zero degrees kelvin (valence band), is separated from a band which is completely empty at zero degrees kelvin (conduction band) by a narrow region of forbidden energies called the energy gap. An energy band diagram of a pure semiconductor at absolute zero is shown in Fig. 3.1. At absolute zero a semiconductor is a perfect insulator, since no partially filled bands exist. At higher temperatures electrons in the valence band may acquire enough thermal energy to be excited across the energy gap and become conduction electrons in the conduction band. The empty states which were left behind also contribute to the conductivity since they represent available energy levels within the valence band. It is evident, then, that as the temperature increases, the number of conduction electrons and the number of holes will increase as will the electrical conductivity.

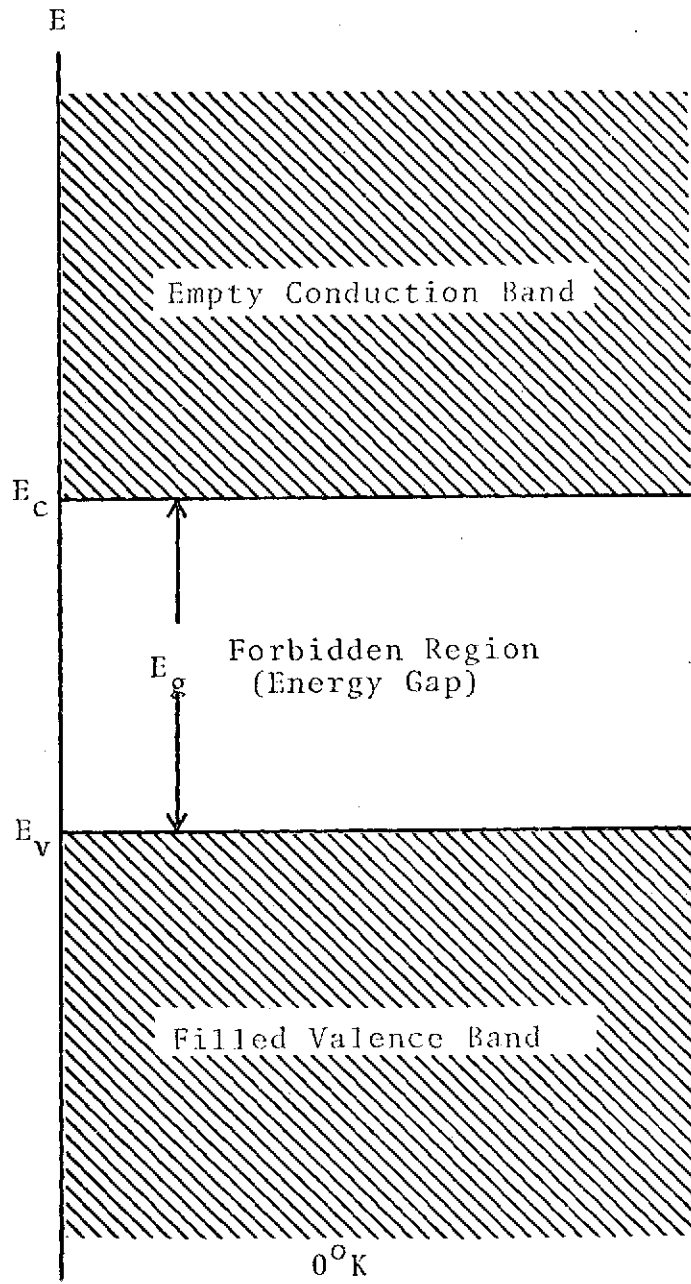


Figure 3.1. Energy Band Diagram of a Pure Semiconductor at 0°K

A semiconductor in which the electrons and holes are created entirely by thermal excitation across the energy gap is called an intrinsic semiconductor. In order to discuss how these particles are distributed in energy, we need to say something about the density of states function. If we let $f(E)$ denote the average number of particles that occupy a quantum state of energy E , and let $g(E)dE$ denote the number of quantum states whose energies lie in a range between E and $E+dE$, then the number of particles whose energy is in the range between E and $E+dE$ is given by

$$N(E)dE = f(E)g(E)dE \quad (3.1)$$

where $f(E)$ is called a distribution function. Since free electrons in semiconductors obey Fermi-Dirac statistics, the distribution function $f(E)$ becomes

$$f(E) = \frac{1}{1 + e^{(E-E_F)/kT}} \quad (3.2)$$

Because only one particle may occupy a given quantum state, the value of $f(E)$ at a particular energy is equal to the probability that a quantum state of that energy will be occupied. A plot of the density of states, $g(E)$, as a function of E for an intrinsic semiconductor is shown in Fig. 3.2, with the fermi level lying in the center of the forbidden gap. Now that we have briefly reviewed the band theory concepts of crystalline semiconductors, we can continue our discussion of amorphous semiconductors.

Harrison [20] has described a basic model of the electronic structure of amorphous materials and has shown how the transport properties of the material can be explained in terms of the model. He considers a solid semiconductor which has each atom surrounded tetrahedrally by four nearest neighbors. Disorder is introduced into the solid while retaining the tetrahedral coordination which results in some unfilled or "dangling" bonds that can produce states or traps in the forbidden band. These deviations may also cause localized states to rise into the energy gap from the valence band with the energies of these states depending on the details of the local structure. Harrison states that these energies can be distributed throughout the gap but will be for the most part in the vicinity of the valence and conduction band edges, with states near the center of the gap being localized while those near the band edges will be spread out. The energy states in the "forbidden band" are localized and, although the density of states at these energies may be low, they are not zero. Thus, even if impurities are added, the fermi level at room temperature will shift only slightly and remain in a region where all the states are localized. This is what makes amorphous semiconductors appear to be intrinsic even when they are impure. Keeping in mind the discussion of Harrison and returning to the density of states plot we made earlier for the intrinsic semiconductor (Fig. 3.2), we should be able to modify the density of states plot to include amorphous materials. Instead of being sharp, the conduction and valence bands should tail off into the forbidden gap due to

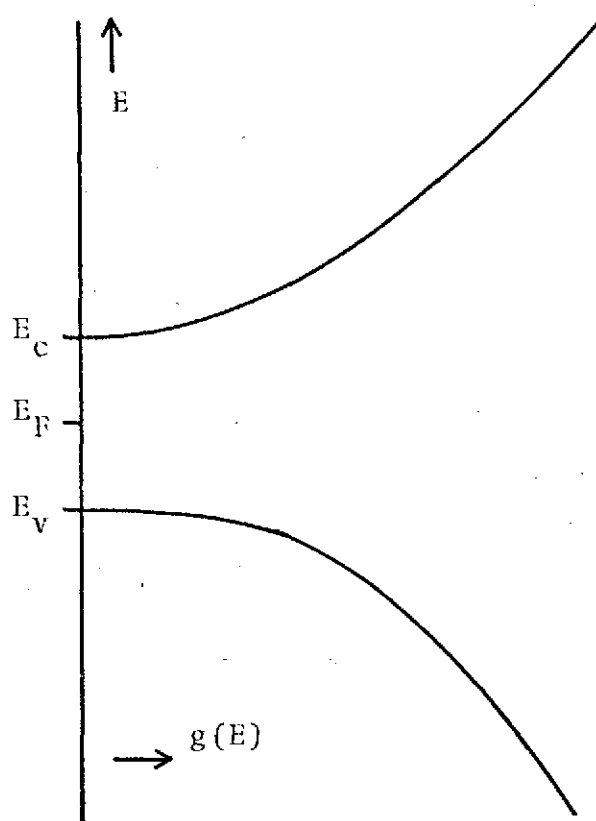


Figure 3.2. Plot of Density of States Versus Energy for an Intrinsic Semiconductor

the presence of the localized states caused by the disorder that was introduced into the material structure, as seen in Fig. 3.3. The short lines that are shown in what was originally the forbidden gap represent trap sites that have been created due to the disorder. The location of the fermi level will depend on the local structure. As the disorder becomes more and more pronounced, these band tails may meet or possibly even overlap. In order to obtain conduction, it is necessary to have electrons in states well above the fermi energy, E_F , or holes in states well below the fermi energy. Since the electrical conductivity cannot be raised significantly by doping, other means have to be considered. One such means is that of injecting large numbers of electrons (or holes) into the material. This can be accomplished by applying a large potential to metal electrodes on the amorphous semiconductor. Harrison suggests that, if the potential is then reduced, electrons could drop from conducting states back into higher-lying traps in the forbidden gap and, at a later time, could be easily reexcited into conducting states, thus causing an occupation of levels in the vicinity of the top of the gap just as if the fermi level had been elevated to that region. The presentation above is analagous to the Ovshinsky effect, which is nothing more than an observed increase in conductivity of an amorphous semiconductor following a pulsed voltage.

Basic Band Model (BBM)

The basic band model was proposed by Mott [7]. He defined an ideal covalent glass as a one, two, or three

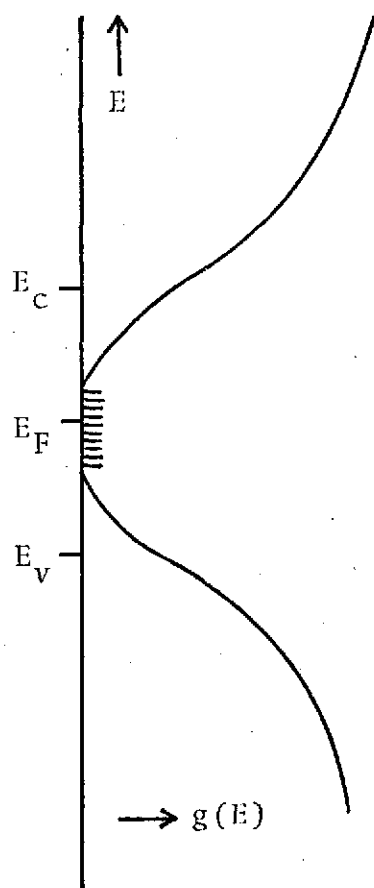


Figure 3.3. Plot of Density of States Versus Energy for an Amorphous Semiconductor

dimensional random network with excellent short-range order and no long-range order. Every atom has its valence requirements locally satisfied with no dangling bonds or structural defects. Mott stated that the following were considered to be basic experimental facts regarding amorphous semiconductors:

1. The electrical conductivity, σ , appears to be primarily intrinsic in its temperature dependence even for alloys of varying valence and different composition.

2. The electrical conductivity has the form

$$\sigma = \sigma_0 e^{-\Delta E / 2k_B T}$$
 over a wide range of temperatures.

3. The pre-exponentials, σ_0 , can be an order of magnitude or more smaller than σ_0 the value for crystals, but the energy gaps are of comparable size.

Mott suggested that defects such as vacancies, dangling bonds, voids, and impurities might lead to nonuniformities in the density of states as seen in Fig. 3.4 and that alloys, because of the presence of both compositional and positional disorder, could lead to an overlapping of the tails in the density of states as seen in Fig. 3.5.

Cohen, Fritzsche and Ovshinsky Model (CFO)

Because chalcogenide glasses may have almost any composition and since disorder has been assumed to have a marked influence on the density of states, extensive tailing can be expected for these materials. Cohen, Fritzsche, and Ovshinsky [7] suggested in their model that the tailing is great enough to make the valence and conduction bands overlap.

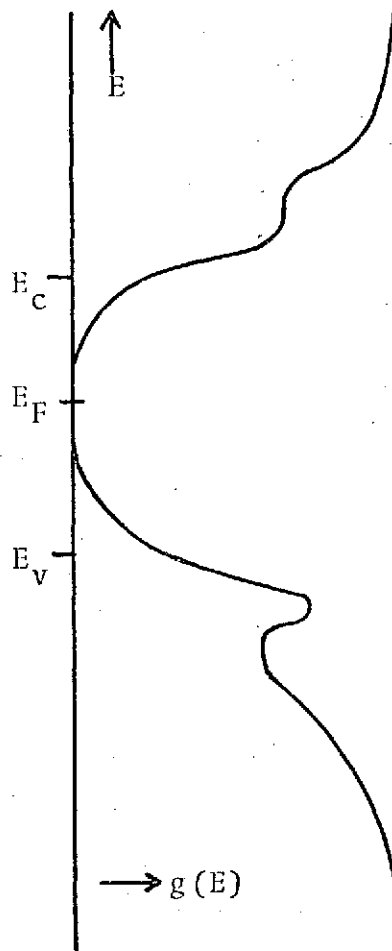


Figure 3.4. Variation of Density of States of an Amorphous Semiconductor Due to Defects Such as Vacancies, Voids, and Impurities

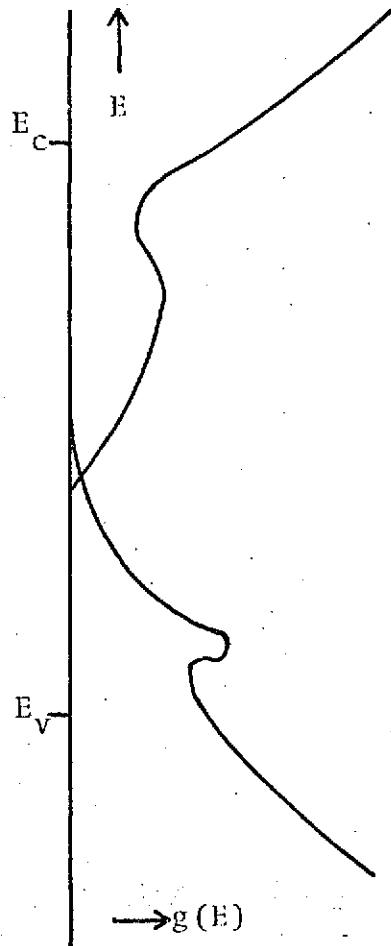


Figure 3.5. Variation of Density of States for Alloys Having Both Compositional and Positional Disorder

A diagram of the Cohen, Fritzsche, Ovshinsky model is shown in Fig. 3.6. Observation of Fig. 3.6 raises two questions:

1. Since the valence and conduction bands overlap, is it possible to make any distinction between them?

2. If states exist in the conduction band with energies that are lower than some of the valence band states, should a repopulation of states take place in order to achieve equilibrium?

Cohen, Fritzsche, and Ovshinsky answer these questions in the following manner. They conclude that a localized state in the valence tail is normally filled, with the corresponding atom being neutral. If the localized state is empty, it represents a positively charged ion. Similarly, a localized state in the conduction tail is generally empty, with the corresponding atom neutral. An electron assuming one of these states would create a negatively charged ion. Thus, there is a distinction between localized states in the two bands. Their answer to the second question is that, provided no donor or acceptor states exist, enough electrons will exist to exactly fill the valence band and leave the conduction band empty. Electrons in higher valence band states may lower their energy by falling into states at the bottom of the conduction band tail. This process continues until the system energy is minimized. Neale [7] has indicated that this model predicts two types of electronic transport: an intrinsic conductivity due to the excitation of electrons above E_c or below E_v (see Fig. 3.6) and a hopping type conductivity among localized states that exist in the gap.

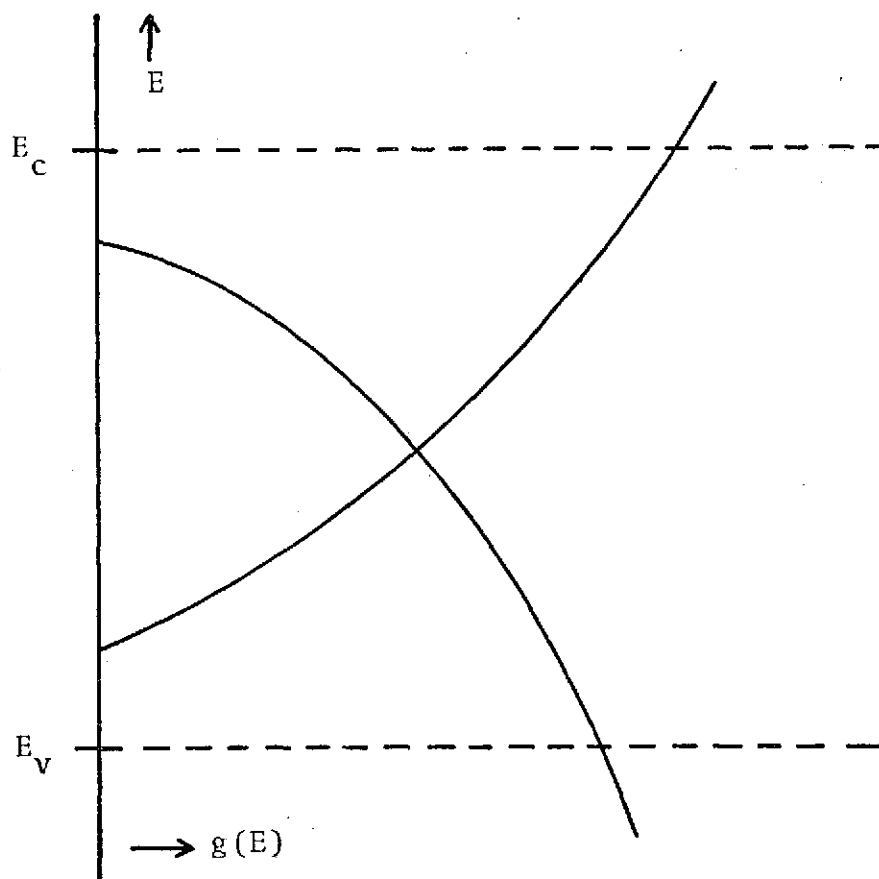


Figure 3.6. The Cohen, Fritzsche, Ovshinsky Model for the Density of States of a Typical Chalcogenide Glass

Henisch, Fagen, and Ovshinsky Model (HFO)

The model proposed by Henisch, Fagen, and Ovshinsky [7] to explain threshold switching is based on double-injection of charge carriers from the electrodes and makes use of the model proposed by Cohen, Fritzsche, and Ovshinsky that was described previously. According to Henisch, Fagen, and Ovshinsky, a negative space charge is formed near the cathode due to the trapping of electrons and, similarly, a positive space charge is formed near the anode. These two space-charge regions limit the current, causing an increase in the electric field in the bulk material. As the two space-charge regions eventually overlap, a region is produced in which all positive and negative traps are filled. Since this region is neutral, it is highly conductive. Electrons will be accelerated toward the anode and holes toward the cathode, and a highly conductive state will form rapidly. The strongest evidence against the charge-injection models for switching is the absence of polarity effects, although some experiments do suggest that at low temperatures some charge-injection processes may play a more dominant role [7].

SUMMARY

Numerous advances have been made recently in trying to understand the structural and electrical properties of amorphous semiconductors. Experimental data has been discussed in terms of mobility gaps and density of states, and a basic band model has been developed. It appears that

several conclusions can be reached about each material investigated, but many difficulties still remain unresolved and a basic simplification of the area is needed.

Producing well-defined reproducible samples for electrical measurements is often impossible. Two sets of films apparently of the same amorphous material could conceivably behave quite differently from each other. It is possible that several different types of metastable disordered structures could be formed from a single chemical composition, depending on the exact preparation technique.

There appears to be one shortcoming in the several models discussed above for threshold switching. Different compositions and different geometries can often lead to different switching mechanisms; therefore, using a given set of data to eliminate a particular model will eliminate it only for that particular case. Although the models presented above resulted from studies of thin film sandwich structures of chalcogenide glasses, the results should be applicable for devices fabricated in a planar structure.

Thermal runaway resulting from rapid Joule heating has long been a frequent explanation of threshold switching. The thermal model accounts for filament formation, the pre-switching delay time, and the negative resistance region. At present, switching seems to be thermally induced for bulk samples and for films thicker than about eight microns. Thermal runaway has been observed in thin films for particular compositions and geometries.

The thermal model as shown in Fig. 3.7 interprets the switching action as arising solely from the heating/conductivity cycle. In many of the thin film devices used in experimental work, it is difficult to separate field and temperature phenomena because the devices switch at voltages where the field and temperature contributions to the conductivity increase and have similar magnitudes.

A number of electronic processes have been suggested as applicable to threshold behavior and behavior in the "on" state of chalcogenide glasses, but none has been developed to the stage where quantitative calculations and predictions can be made. The proposed models make few concessions to the amorphous nature of the material. The chalcogenide glass is often regarded as a typical semiconductor modified only by the presence of a larger than normal density of traps and/or recombination centers.

There is surprisingly little published data on the I-V characteristics of the kind of chalcogenide glass compositions generally used in switching devices.

A large amount of the published data is essentially concerned with the same type of device using basically the same or similar compositions. It is, therefore, difficult to be sure whether the data are typical or peculiar to that particular form of device.

Electronic processes make an important contribution to the non-ohmic conductivity of chalcogenide glasses in the preswitching region, but none of the models seems to give an

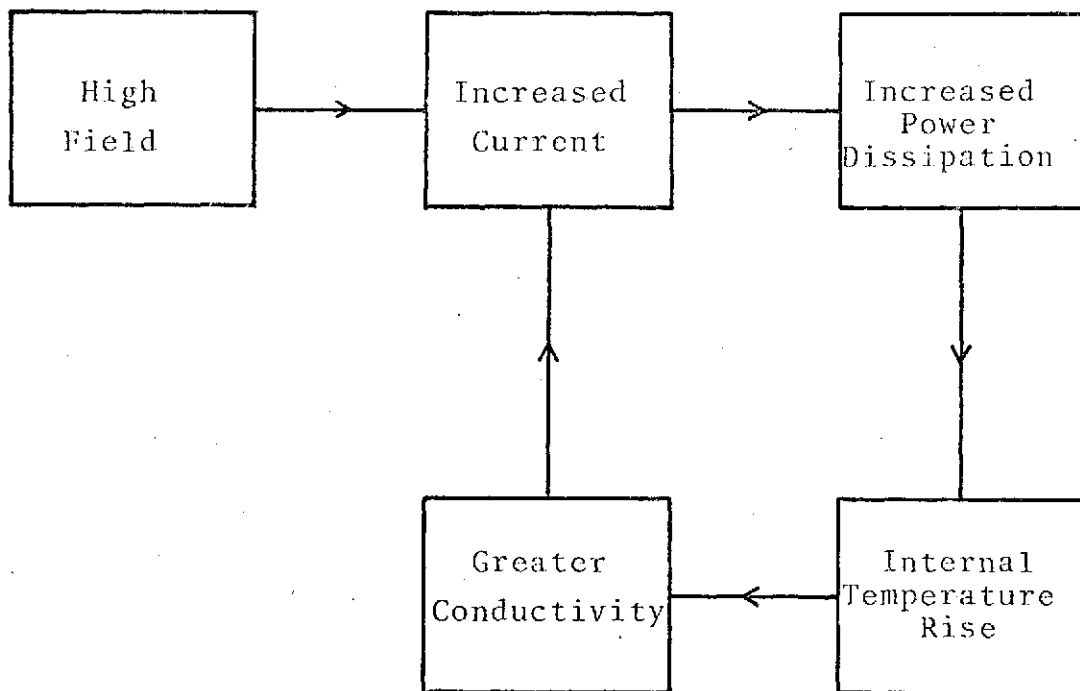


Figure 3.7. The Thermal Model of Threshold Switching

adequate account of this, at least not in its elementary form. For smaller electrode separations, there appear to be significant changes in the temperature and thickness dependence of threshold voltage and this is generally accepted as evidence that electronic effects are predominant. Experiments to measure the threshold voltage as a function of electrode spacing are difficult to perform. It is obviously necessary to maintain both materials and boundary conditions while varying the electrode spacing. Since the threshold voltage depends on the immediate history of the applied voltage and the temperature, the threshold voltage should be measured by applying a slowly varying voltage to the device.

At the present time models and theories of high-field phenomena are not developed well enough to apply confidently to complex switching processes. Discrimination between the thermal and electronic models appears to require the measurement of device temperatures during the switching actions. Thus, at the present time, one can only speculate on the relationship between the behavior in the preswitching region and the actual threshold conditions.

CHAPTER 4

EXPERIMENTAL PROCEDURE

FILM FABRICATION

The thin-film silver-SnSe devices used for this investigation were vacuum deposited. Figure 4.1 shows a cross-sectional view of two typical devices. The devices were planar and consisted of a layer of SnSe overlain with silver contacts or silver contacts overlain with SnSe. The materials were evaporated by means of an electron beam gun system and the deposition parameters were controlled by a Sloan Omni II unit. Figure 4.2 shows a schematic of the vacuum evaporation system used in this investigation. In this system the kinetic energy acquired by the electrons as they leave the filament of the gun is converted to heat upon striking the surface of the material being deposited. This heat raises the temperature of the material, thus causing it to evaporate. The evaporated material leaves the surface in all directions and condenses through a mask pattern onto the substrate above.

All depositions were made on glass substrates which were cleaned by the same process as that described by Yen[21]. After completing the cleaning procedure, the substrates were visually inspected and immediately loaded into the vacuum

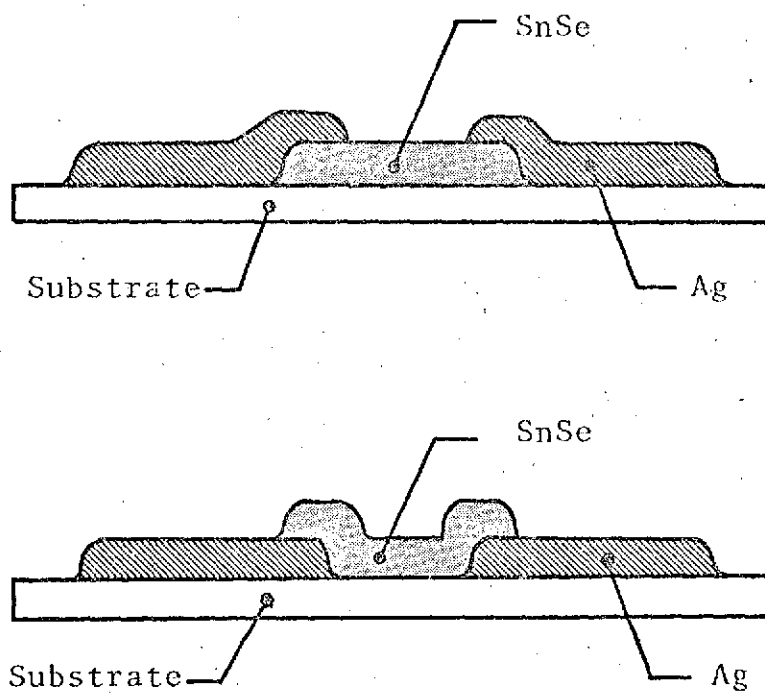


Figure 4.1. Cross Section View of Typical Ag-SnSe Devices

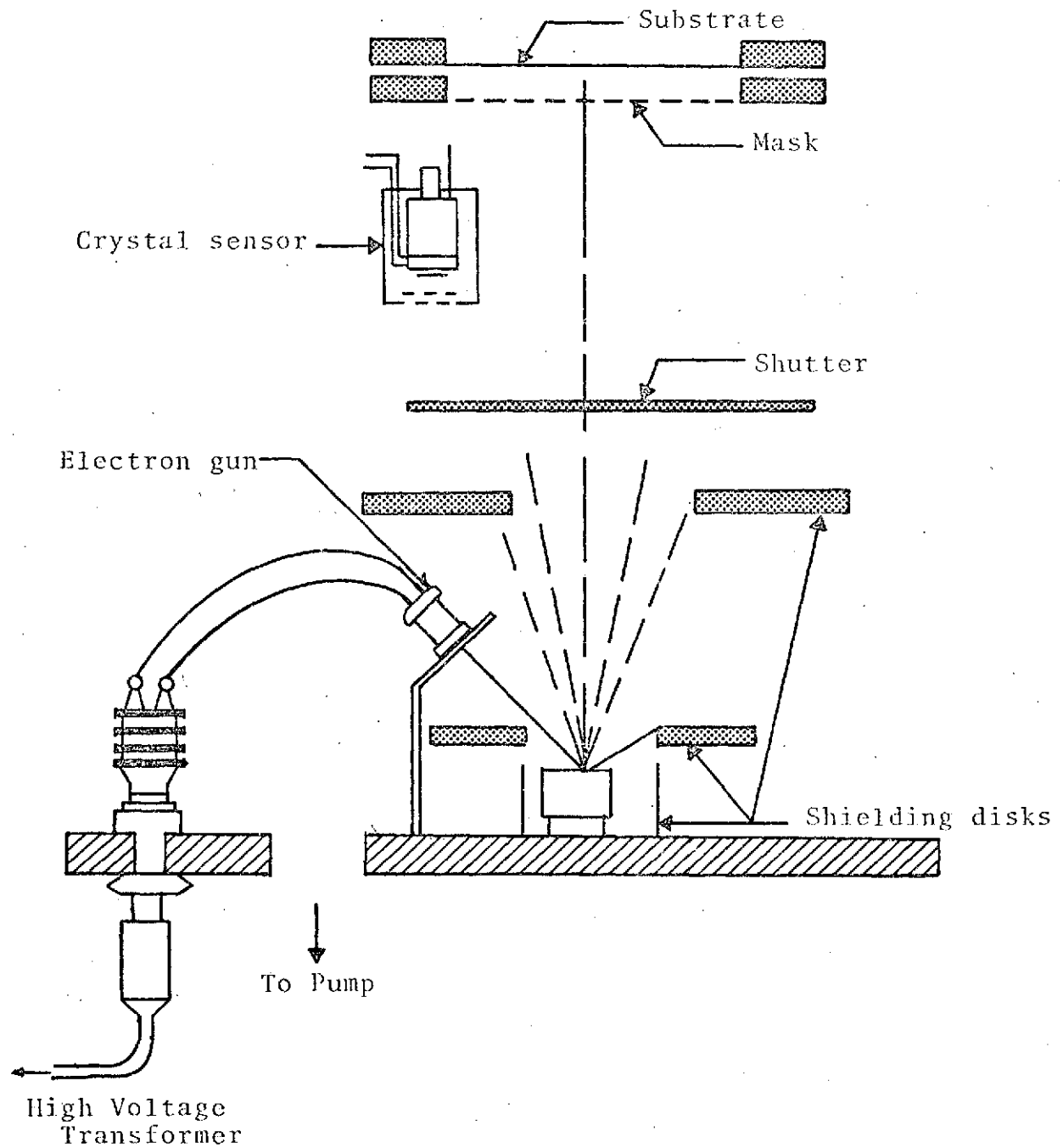


Figure 4.2. Vacuum Evaporation System for Deposition of Materials

system. A mechanical and oil diffusion pump were then used to evacuate the system to a pressure of approximately 10^{-6} Torr.

A quartz crystal oscillator, connected to the Sloan Omni II, was used to give a continuous reading of the thickness of the films being deposited. The quartz crystal received a deposit of material at the same time as the substrates. This deposited material resulted in a change in the natural resonant frequency of the crystal. The total change in frequency during deposition is proportional to the mass of the material deposited on the crystal and, therefore, a measurement of the change in frequency allows one to determine the thickness of the deposited films. To correlate the frequency shift with film thickness, silver and tin selenide films of varying thickness were deposited and the corresponding frequency shifts recorded. The film thicknesses in angstroms were measured with a multiple beam interferometer and calibration curves for thickness as a function of frequency shift were obtained (see Fig. 4.3). From this point on, the assumed film thicknesses were based entirely on the measured frequency shifts.

Initial devices used in this investigation were fabricated using the mask patterns shown in Fig. 4.4, whereas the patterns shown in Fig. 4.5 were used in subsequent devices. All mask patterns used in this study were made of beryllium copper using the process previously described by Baxter[22].

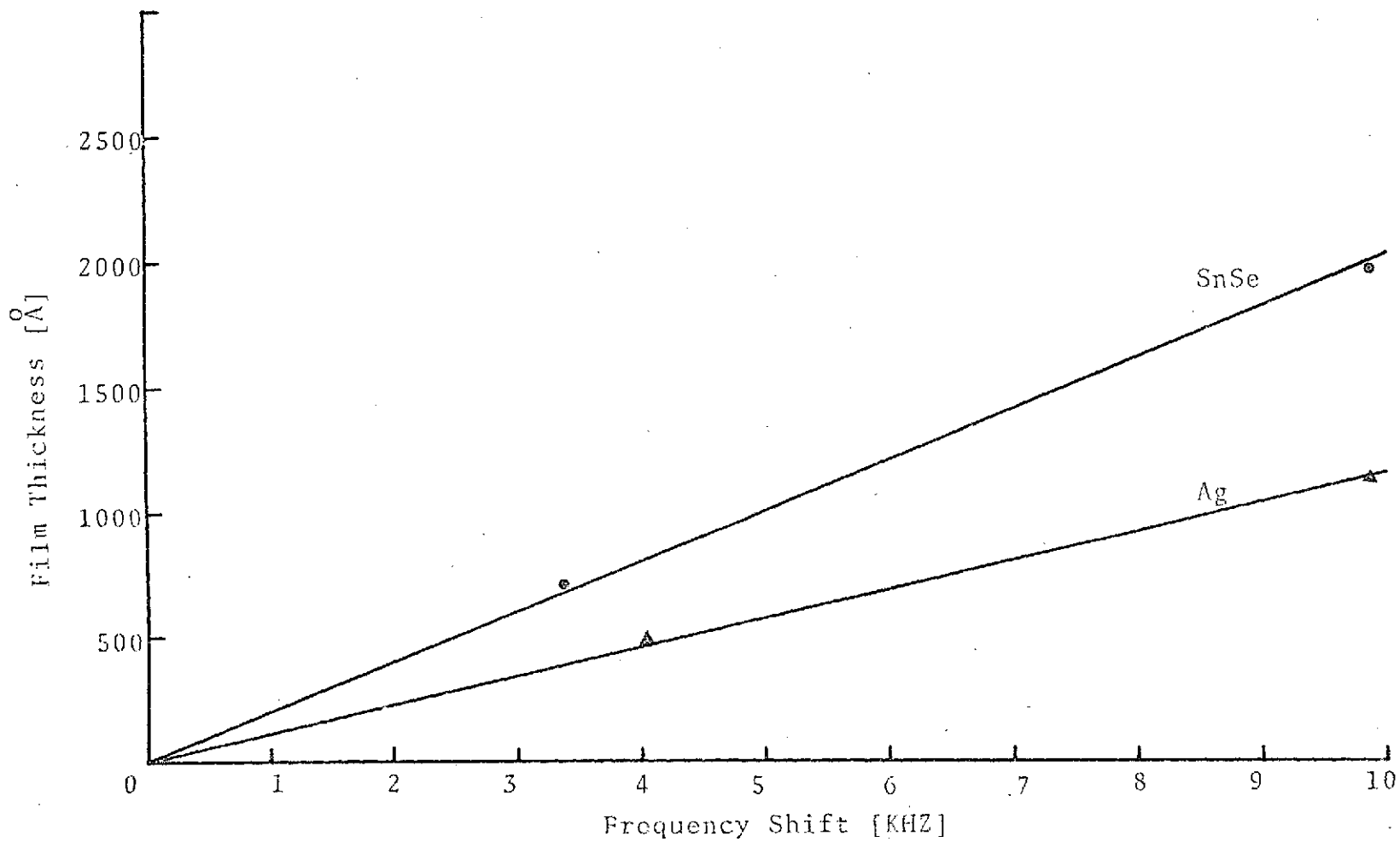


Figure 4.3. Calibration Curves for the Deposition of Ag and SnSe

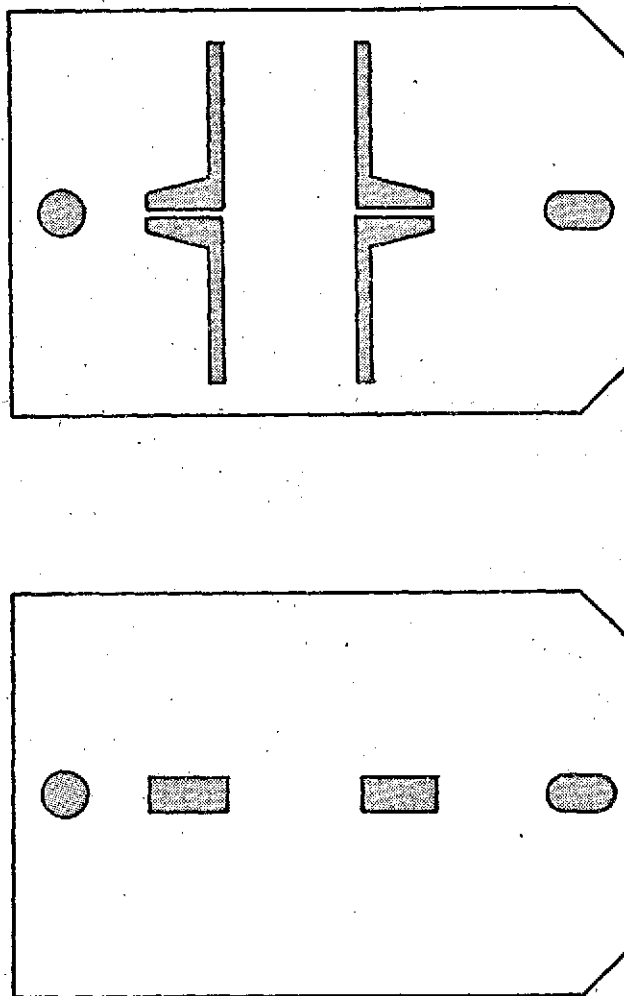
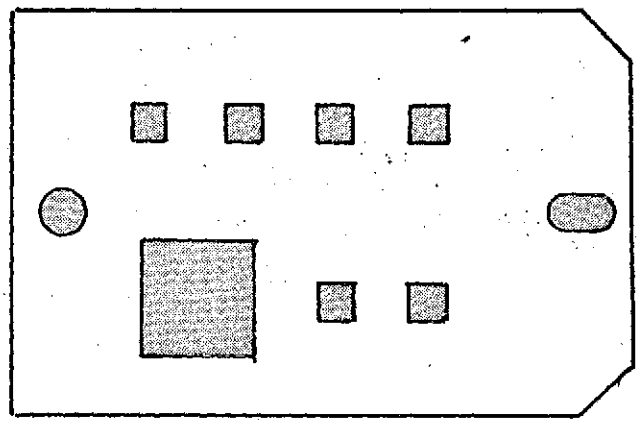
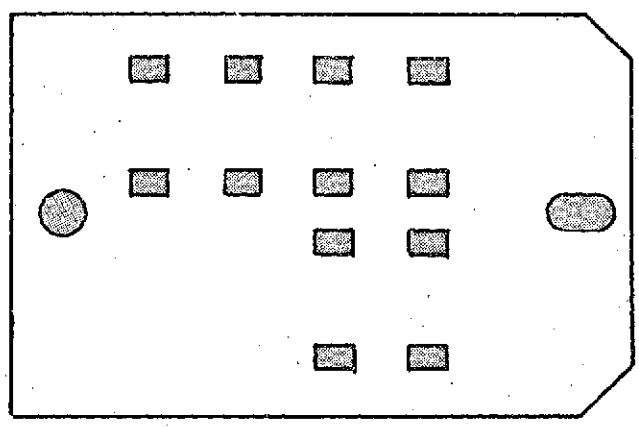


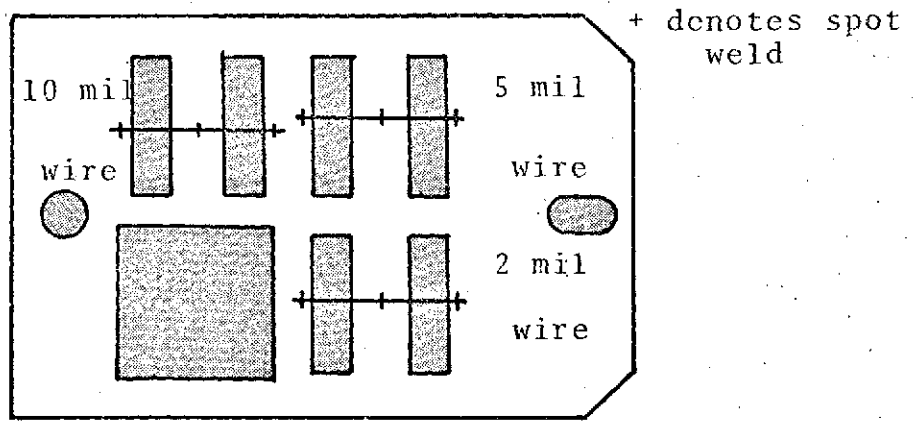
Figure 4.4. Mask Patterns Through Which Initial Films Were Evaporated



(c)



(b)



(a)

Figure 4.5. Mask Patterns Used in Fabricating Final Devices

Using the mask patterns shown in Fig. 4.5, it was possible to fabricate six devices at one time. As seen in Fig. 4.5a, the devices were divided into three groups by spot welding a 2, 5 and 10 mil wire onto the beryllium-copper to define electrode separation. A thin layer of silver deposited at a low rate was used to define the electrode spacing. The low deposition rate was necessary in order to reduce the possibility of the gaps being shorted out by the diffusion of material around the wires. Solder pads were formed by depositing additional silver through the pattern shown in Fig. 4.5b and, finally, the active material (SnSe) was deposited using the mask pattern shown in Fig. 4.5c.

During the fabrication process for the last several series of devices, the rate of deposition of the tin selenide was monitored with a minicomputer interfaced to a data acquisition system, high speed digital plotter, and high speed reader/punch. A block diagram of the monitoring system is shown in Fig. 4.6. The rate was monitored at one second intervals and the corresponding values stored in the computer memory. Since the minicomputer contains a limited amount of memory, the monitoring time was limited to approximately ten minutes. Once the monitoring cycle was completed, the rate was plotted as a function of time and a punched paper tape of the data for later use was obtained.

Difficulty was encountered in attempting to control the rate at which the tin selenide films were deposited. Fig. 4.7 and Fig. 4.8 show deposition rate versus time plots

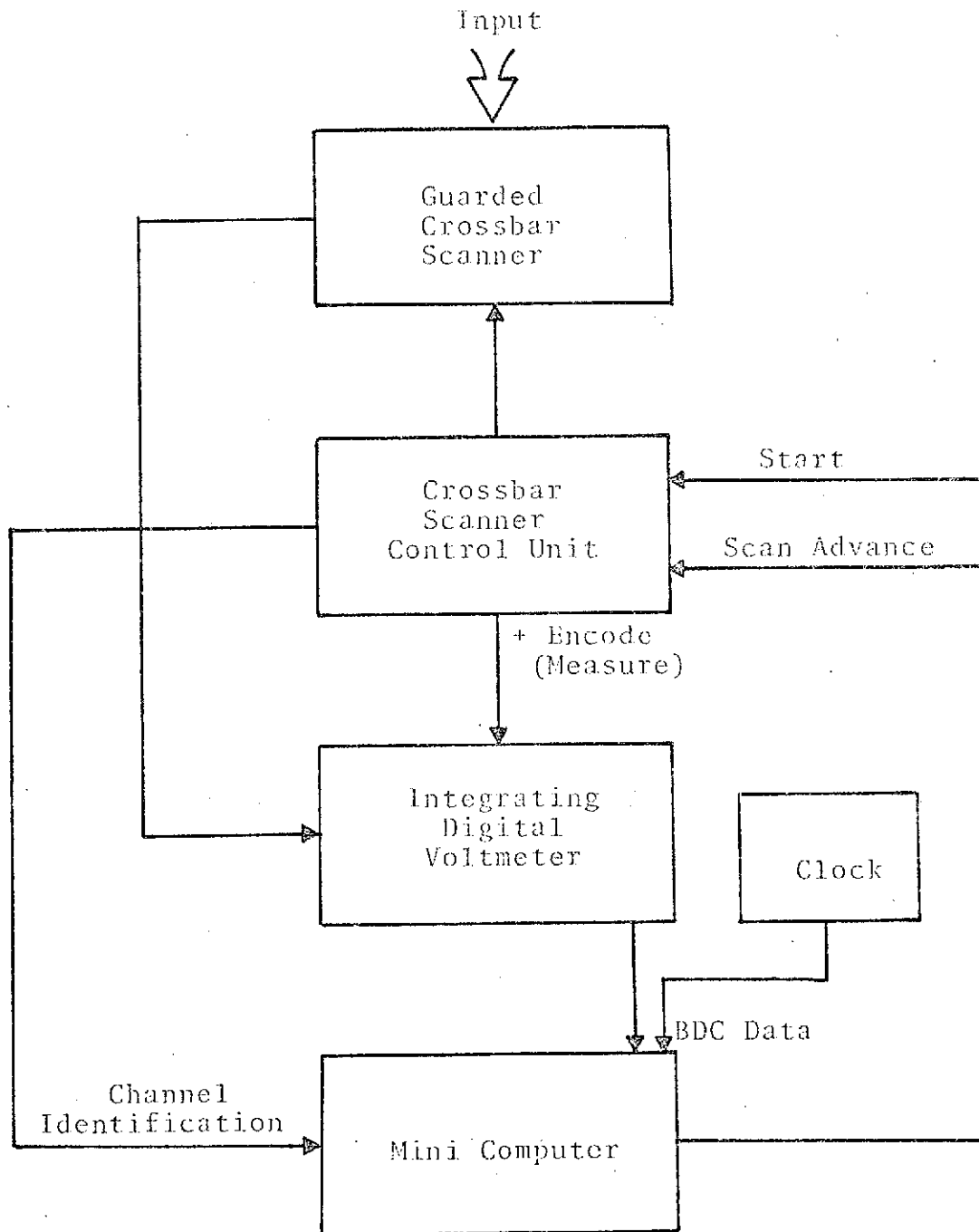


Figure 4.6. Block Diagram of Data Acquisition System

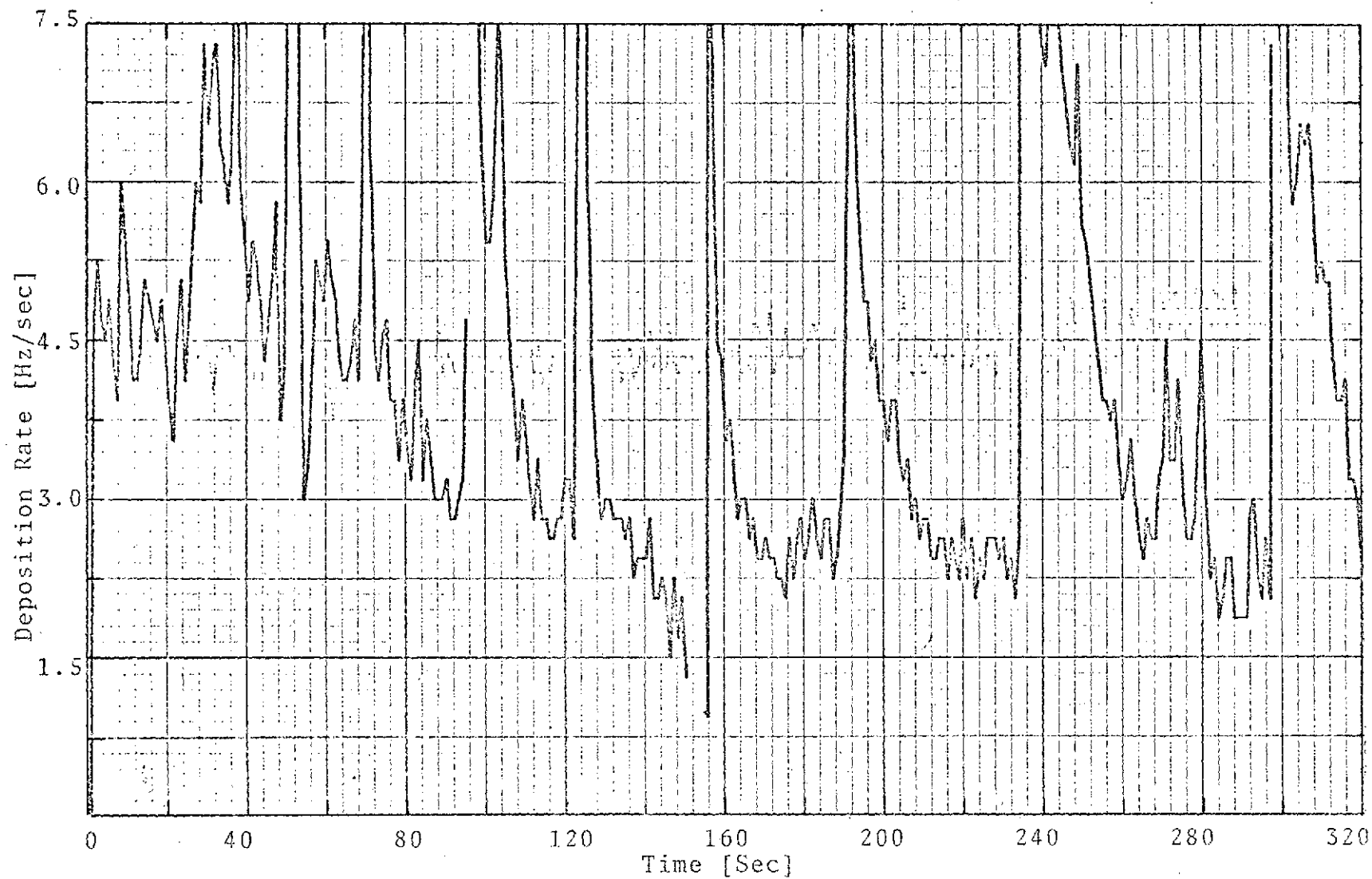


Figure 4.7. Variations in Deposition Rate Typical of Materials Obtained from Source A

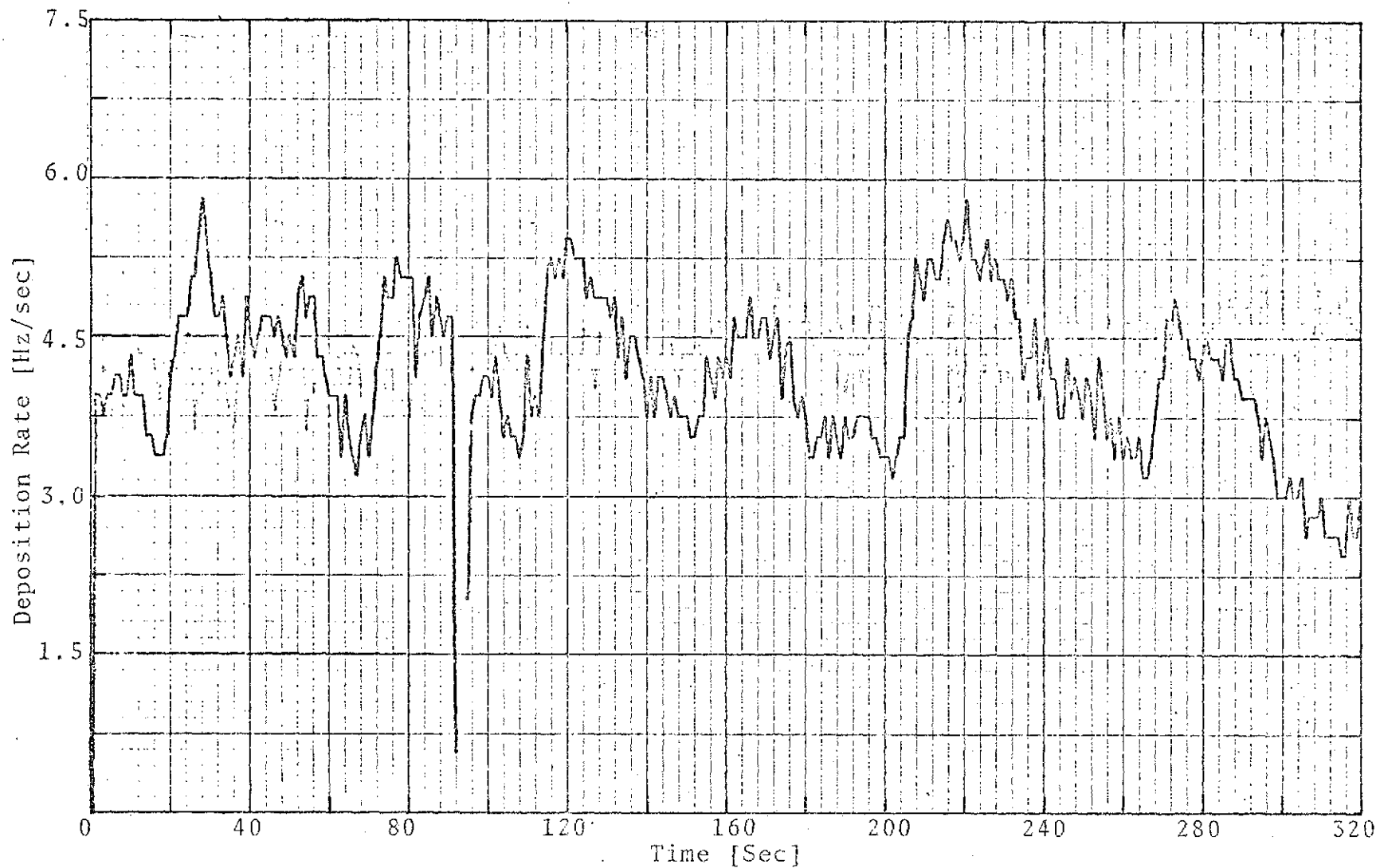


Figure 4.8. Variations in Deposition Rate Typical of Materials Obtained from Source B

for tin selenide obtained from two different suppliers. Rate fluctuations of this type can have a marked effect on the properties of the final film, especially with a low melting temperature material such as tin selenide. Since SnSe is a compound, it is desirable to deposit this material at a slow, controlled rate in order to keep the material from decomposing and yielding a tin-rich or selenium-rich film. Efforts are presently underway to allow a minicomputer to have control over the rate of deposition, but this project was not advanced enough for use with this study.

FILM TEST PROCEDURES

To test the devices for possible memory switching characteristics, a series of voltage pulses of varying height, width, and decay time was applied to the devices and the resistance was measured after each applied pulse. Initial devices were tested using a signal generator with a push button switch to initiate the pulses. The voltage drop across the sample and the voltage drop across a fixed resistor in series with the sample were displayed on a dual trace storage oscilloscope. These voltage drops along with the value of the series resistor were used in calculating the sample resistance. With the signal generator used, there was no way to obtain pulses with a trailing edge, that is, a finite decay time. To overcome this problem a multiposition rotary switch was wired with different resistance-capacitance combinations in order to obtain different decay times.

Because of the large amount of time involved in the above testing procedure and since the pulses that were attainable were not of sufficient magnitude to obtain switching in many of the films, an automated testing procedure was developed. This technique was somewhat elaborate as it involved the interconnection of a digital to analog converter (D/A), minicomputer, data acquisition system, high speed digital plotter, high speed reader/punch, and a linear amplifier using a μA 741 operational amplifier.

The 12 bit D/A converter used took a digital input between zero and 4096 (2^{12}) and yielded a proportional analog output between zero and 9.99 volts. By setting the D/A to a desired value, leaving it on for a predetermined time, and controlling how fast it turned off, rectangular pulses of varying height, width, and decay time were obtained. Since the maximum output voltage obtainable from the D/A was 9.99 volts, it was necessary to use a linear amplifier in order to achieve the desired voltage levels. The output of the amplifier was connected to a series combination of a fixed resistor and the device to be tested. A schematic diagram of this arrangement is shown in Fig. 4.9.

A computer program which caused the D/A converter to generate a series of rectangular pulses of varying height, width, and decay time was written to control the testing procedure. These pulses were then amplified and applied to the series combination of sample and fixed resistor. A small leakage current ($<10 \mu\text{a}$) flowed through the fixed resistor

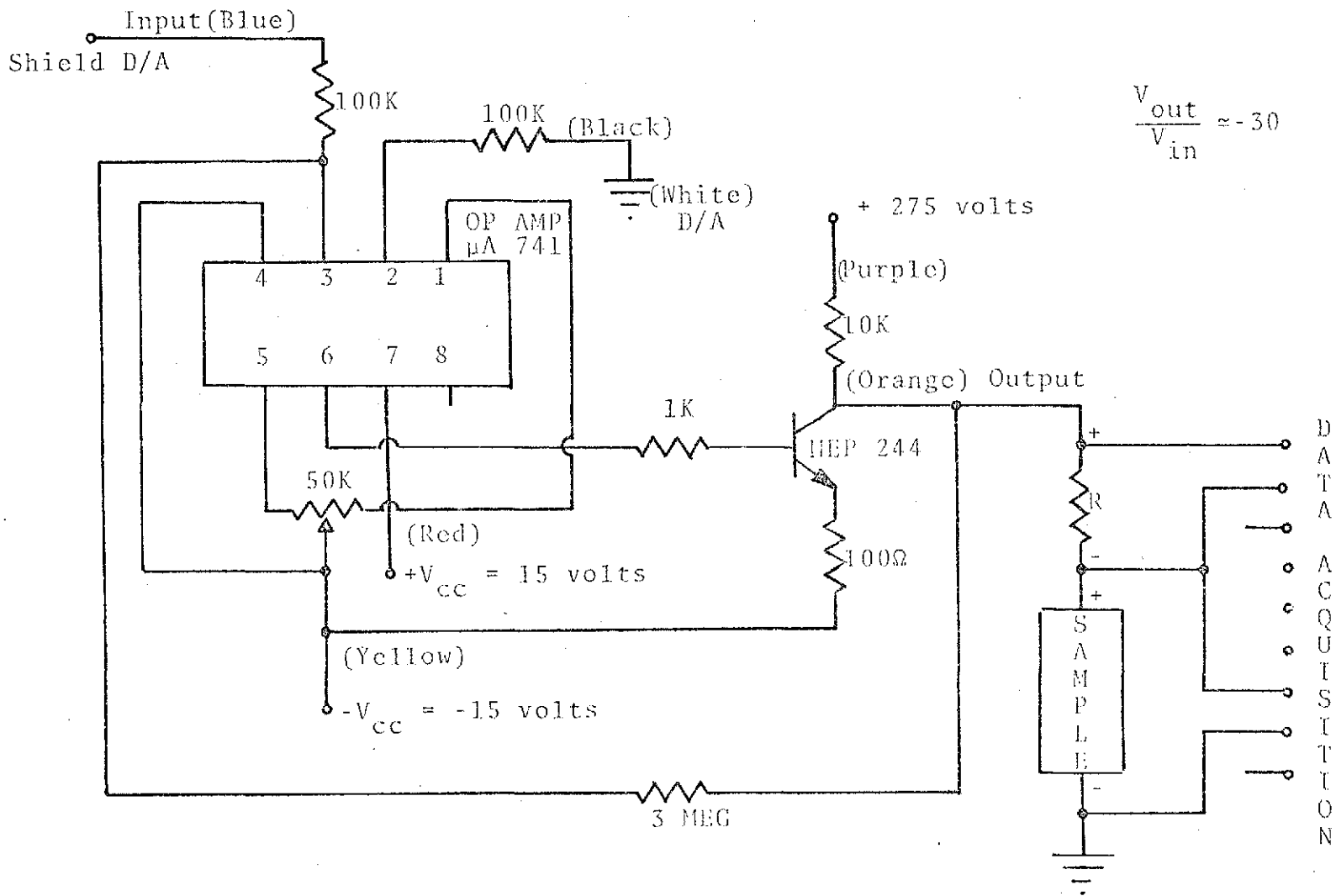


Figure 4.9. Schematic Diagram of Linear Amplifier Circuit

and device with no pulses applied. The voltage drop across the device and the voltage drop across the fixed resistor were measured using the data acquisition system. After the application of each pulse, the data obtained was punched out on the high speed punch for possible use at a later date; the sample resistance, pulse height, pulse width and decay time were plotted on the high speed digital plotter and a tabular listing of the applied pulses and associated resistances were printed on the teletype. The computer then waited for a specified number of seconds before applying the next switching pulse. The purpose of this delay was to allow time for the dissipation of heat generated in the sample by the applied pulse. A sample of the printed output and a sample plot are shown in Table 4.1 and Fig. 4.10, respectively.

The computer program was set up in such a way that, if the device switched from a high impedance to a low impedance state, the bell on the teletype would ring several times and either of two options were available. The resistance in this state could be monitored for any given number of times or a subroutine could be initiated which would try to switch the device back to its high impedance state by applying a series of pulses having a sharp cutoff.

To test the devices for threshold behavior, they were connected to a transistor curve tracer. The voltage across the device was increased gradually and the voltage-current characteristic displayed was visually observed for any abrupt changes in slope caused by the sample switching

Table 4.1. Sample of Output Data Obtained
During Sample Testing

SAMPLE: 4 / 16 / 74 / 2.31
 TEST DATE: 4 / 17 / 74 / 1
 VALUE OF SERIES RESISTOR IS 10000 OHMS
 SIZE OF GAP IS 10 MILS

SAMPLE RESISTANCE (OHMS)	PULSE HEIGHT D/A(VOLTS)	PULSE WIDTH (SECONDS)	DECAY TIME (SECONDS)
7094145			
7122739	.5	.0005	.02
7134110	.5	.001	.02
7185314	.5	.002	.02
7239563	.5	.004	.02
7282159	.5	.008	.02
7303567	.5	.016	.02
7332271	.5	.032	.02
7341312	.5	.064	.02
7349657	.5	.128	.02
7367252	.5	.256	.02
7371855	.5	.512	.02
7361499	1	.0005	.02
7343591	1	.001	.02
7332227	1	.002	.02
7345301	1	.004	.02
7328028	1	.008	.02
7337389	1	.016	.02
7300596	1	.032	.04
7297422	1	.064	.04
7285526	1	.128	.04
7282790	1	.256	.04
7261070	1	.512	.04
7241530	1.5	.0005	.02
7215375	1.5	.001	.02
7215421	1.5	.002	.022
7212214	1.5	.004	.02
7196604	1.5	.008	.02
7183793	1.5	.016	.02
7154195	1.5	.032	.06
7166703	1.5	.064	.06
7141717	1.5	.128	.06
7119811	1.5	.256	.06
7146189	1.5	.512	.06

Table 4.1. (continued)

Sample Resistance (Ohms)	Pulse Height D/A(Volts)	Pulse Width (Seconds)	Decay Time (Seconds)
7082101	2	.0005	.02
7055259	2	.001	.02
7060755	2	.002	.02
7018436	2	.004	.02
7005285	2	.008	.02
7027307	2	.016	.02
6998942	2	.032	.08
6988814	2	.064	.08
6971212	2	.128	.08
6996201	2	.256	.08
7033135	2	.512	.08
6916893	2.5	.0005	.02
6890252	2.5	.001	.02
6860244	2.5	.002	.02
6871508	2.5	.004	.02
6844692	2.5	.008	.02
6836638	2.5	.016	.02
6820819	2.5	.032	.1
6840272	2.5	.064	.1
6828624	2.5	.128	.1
6855019	2.5	.256	.1
6903454	2.5	.512	.1
6752647	3	.0005	.02
6730527	3	.001	.02
6711593	3	.002	.02
6713072	3	.004	.02
6678140	3	.008	.02
6685461	3	.016	.02
6675502	3	.032	.12
6686781	3	.064	.12
6685939	3	.128	.12
6724438	3	.256	.12
6810433	3	.512	.12
6603383	3.5	.0005	.02
6577236	3.5	.001	.02
6557354	3.5	.002	.02
6536143	3.5	.004	.02
6536489	3.5	.008	.02
6545544	3.5	.016	.02
6541938	3.5	.032	.14
6558876	3.5	.064	.14
6546656	3.5	.128	.14
13709.65	3.5	.256	.14
5537.209	3.5	.512	.14

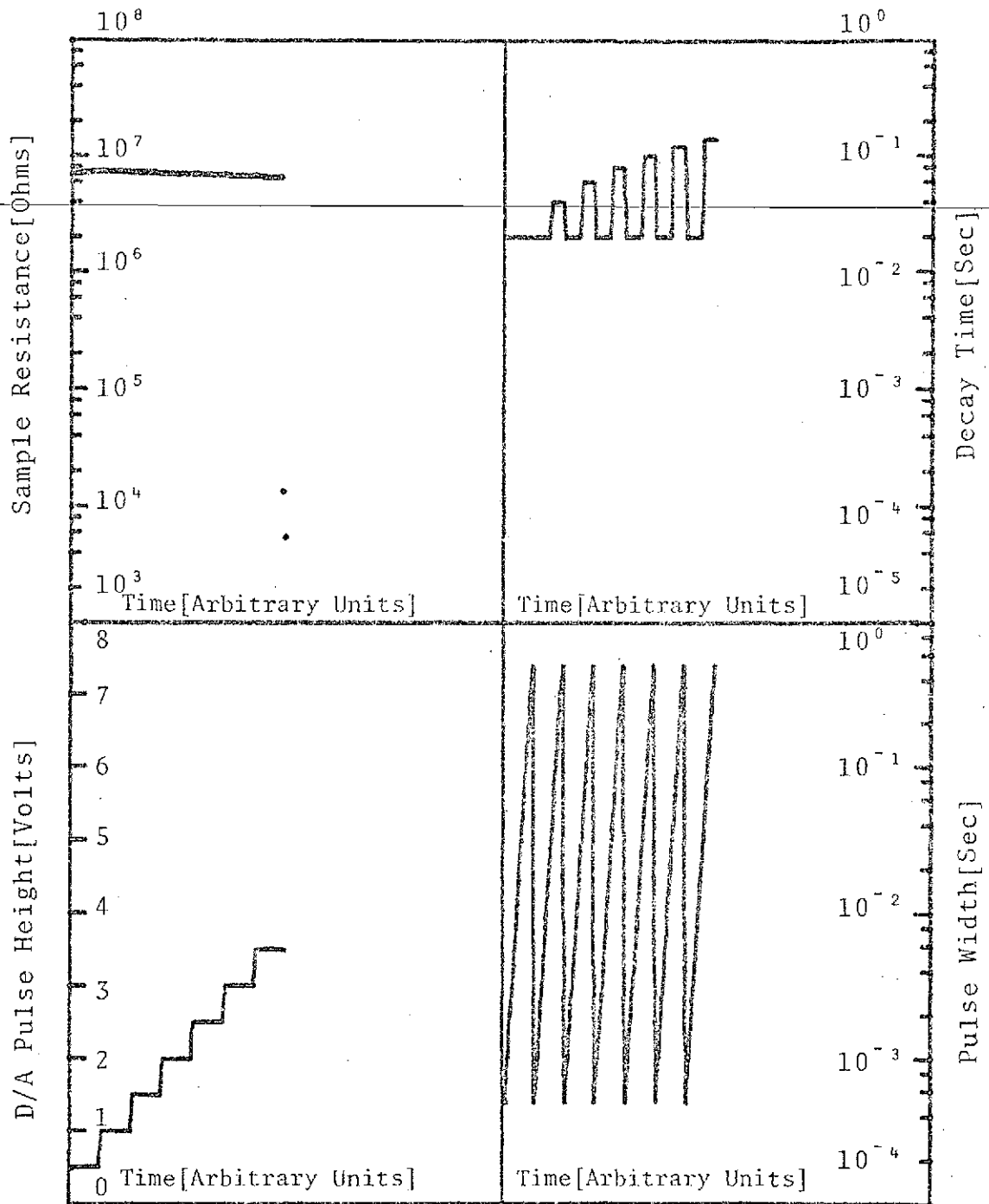


Figure 4.10. A Sample Plot of Data Obtained During a Test Cycle

from a high to a low impedance state. Several samples were tested in this manner and an irreversible process was observed; that is, at certain voltage levels, some of the devices exhibited an abrupt change in resistance but, as the voltage was slowly decreased, the samples remained in their low resistance state. Since no indication of threshold switching was observed, further testing for this mode of switching was discontinued and all of the effort was concentrated on checking the devices for memory characteristics.

During this investigation the fabrication and testing procedures were modified several times in an effort to obtain information that would be beneficial in the final analysis. As mentioned previously, the initial manual testing procedure was replaced with an automated process because of the time involved in making the measurements and, also, because of the inability to obtain sufficient magnitudes of pulse height, pulse width, and decay time. Earlier devices were fabricated as shown in Fig. 4.1 with a fixed electrode spacing (gap width) of 10 mils. Later devices were fabricated using the patterns shown in Fig. 4.5 so that devices could be deposited under essentially the same conditions with the only variable being the gap width. This was done in an effort to check the correlation between the switching characteristics observed and the electrode separation.

During the entire investigation approximately 120 devices were fabricated, of which about 60 showed some indication of changing resistance. This remark, however, should

not be taken to mean that the other films did not possess switching properties. The testing procedure was set up to take devices which were initially in a high resistance state (typically greater than 100 k Ω) and switch them into a low resistance state. Some devices had initial resistances that were too low to warrant testing although, during the latter part of the study, devices that were in an initial low impedance state were able to be switched between two stable resistance states. This will be discussed further in the next chapter.

Several problems were encountered in obtaining films with suitable base resistances. Some samples were shorted due to the diffusion of material around the wires defining the gaps or because the spot-welds had broken loose on the mask pattern. Another problem was encountered when the SnSe film was deposited first, followed by the Ag contacts. When the contact pattern was mated with the substrate during the deposition process, the wires on the contact pattern would scratch the SnSe film and cause open circuit conditions to exist. This problem was eliminated by putting the contacts down first, followed by the tin selenide. The above reasons account for the high attrition rate among the 24 devices listed in Table 4.2. Thus, in most of the final devices that were tested, those films which had suitable base resistances showed some evidence of changing resistance. The devices listed in Table 4.2 are representative of the final devices

Table 4.2. Samples Used for Comparison of Switching Characteristics

Sample Number	Thick-ness (Angstroms)	Gap Width (Meters)	Switching Observed	Low Initial Resistance
A1	580	0.0000508	No	Yes
A2	580	0.000127	No	Yes
A3	580	0.000254	Yes	No
B1	580	0.0000508	No	Yes
B2	580	0.000127	No	Yes *
B3	580	0.000254	No	No **
C1	580	0.0000508	Yes	No
C2	580	0.000127	Yes	No
C3	580	0.000254	Yes	No
D1	650	0.0000508	No	Yes *
D2	650	0.000127	No	Yes
D3	650	0.000254	Yes	No
E1	1350	0.0000508	Yes	No
E2	1350	0.000127	Yes	No
E3	1350	0.000254	Yes	No
F1	1350	0.0000508	No	Yes *
F2	1350	0.000127	Yes	No
F3	1350	0.000254	Yes	No
G1	1350	0.0000508	No	Yes *
G2	1350	0.000127	No	Yes *
G3	1350	0.000254	Yes	No
H1	1350	0.0000508	No	Yes *
H2	1350	0.000127	Yes	No
H3	1350	0.000254	No	No

* Possible Shorted Gap

** Possible Open Gap

fabricated in this study. An analysis of the data obtained from these samples will be discussed in a later section.

ANALYSIS PROCEDURE

Due to the large number of variables involved in this study, the correlation procedures were long and tedious. In order to determine when and under what conditions the SnSe films exhibited switching properties, it was necessary to take the raw data obtained from the testing procedures described above and correlate it with deposition parameters (rate, thickness, and electrode separation), energy per unit volume applied to the sample during each applied pulse, and switching percentage, which is simply the percentage change in the resistance resulting from each applied pulse. Assuming that the sample resistance is large compared to the 10k Ω series resistor, the energy supplied to the sample by an applied voltage pulse can be expressed as:

$$E_s = \frac{V^2 D}{R} + \frac{V^2 F}{2R} \quad (4.1)$$

where V = height of voltage pulse (volts)

D = width of voltage pulse (seconds)

F = decay time of voltage pulse (seconds)

R = sample resistance prior to applied pulse (ohms)

The quantity S_F is a measure of the percentage decrease in resistance that occurred due to an applied voltage pulse and is given by the expression

$$S_F \equiv \left(\frac{R_1 - R_2}{R_1} \right) \times 100\% \quad (4.2)$$

where R_1 = sample resistance prior to the applied pulse

R_2 = sample resistance after the applied pulse.

Since data tapes had been obtained during the testing procedure as explained in this chapter, computer programs were written that would read the data tapes and calculate S_F , E_S , and E_S/V_S where V_S represents the sample volume. The sample volume was calculated using the expression

$$V_S = WLT \quad (4.3)$$

where W = gap width in meters

L = gap length in meters

T = film thickness in meters.

The gap length for all the samples listed in Table 4.1 was 0.00508 meters. A plot routine was incorporated into the programs to allow the variables to be plotted on the high speed digital plotter.

As explained previously, the output voltage of the D/A converter was used as the input to a linear amplifier in order to obtain the necessary voltage variation during testing. Fig. 4.11 shows the amplifier output voltage versus D/A voltage with the load resistance as a parameter. For analysis purposes, these curves have been approximated with the following equations:

$$V_A = 17.2 V_{D/A} \ln(\ln R) \quad R < 100k \text{ ohms} \quad (4.4)$$

and

$$V_A = 27.7 V_{D/\Lambda} \quad R \geq 100k \text{ ohms} \quad (4.5)$$

where the resistance R in (4.4) is expressed in k ohms:

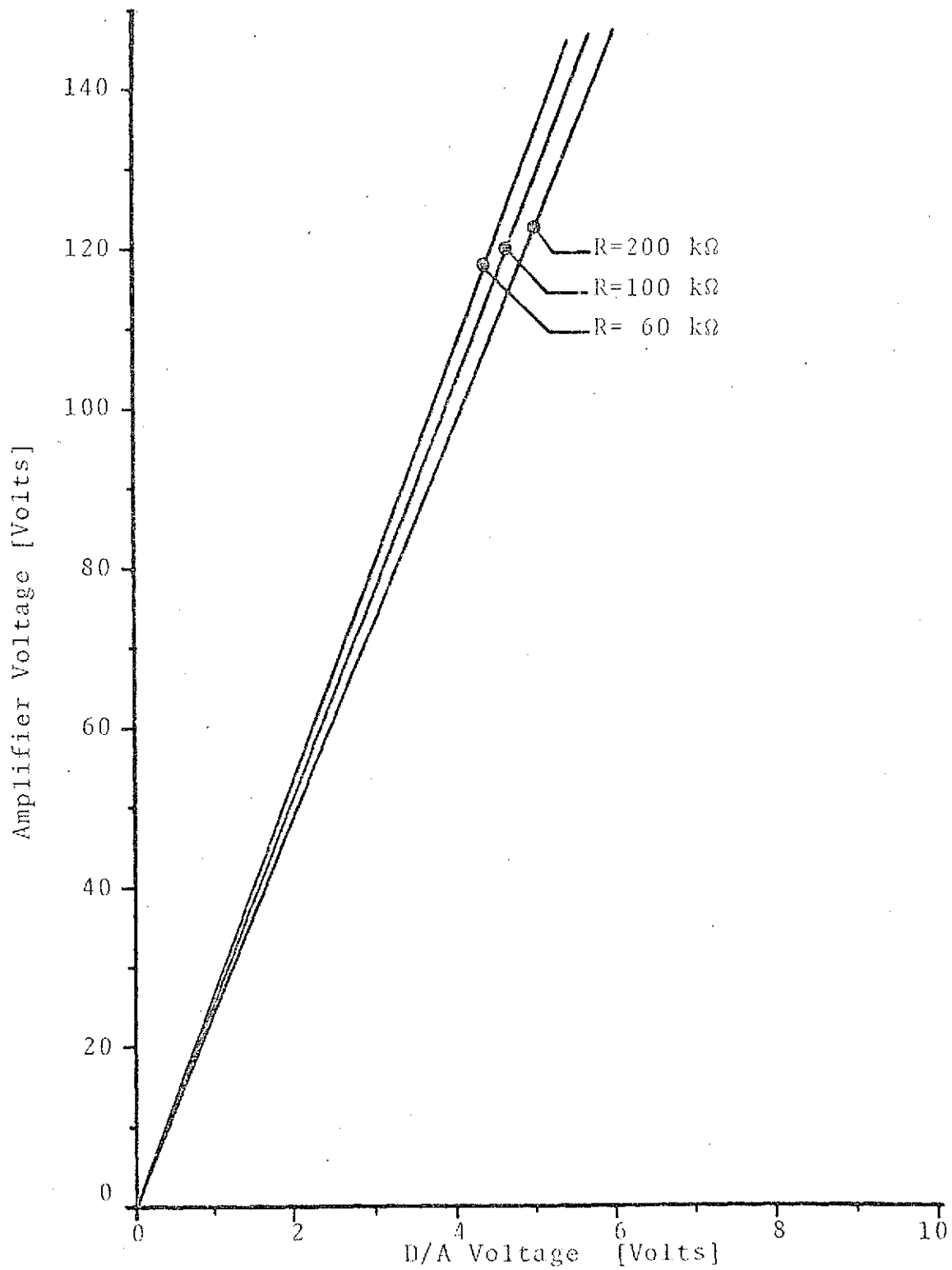


Figure 4.11. Plot of Amplifier Voltage Versus D/A Voltage with the Load Resistance as a Parameter

CHAPTER 5

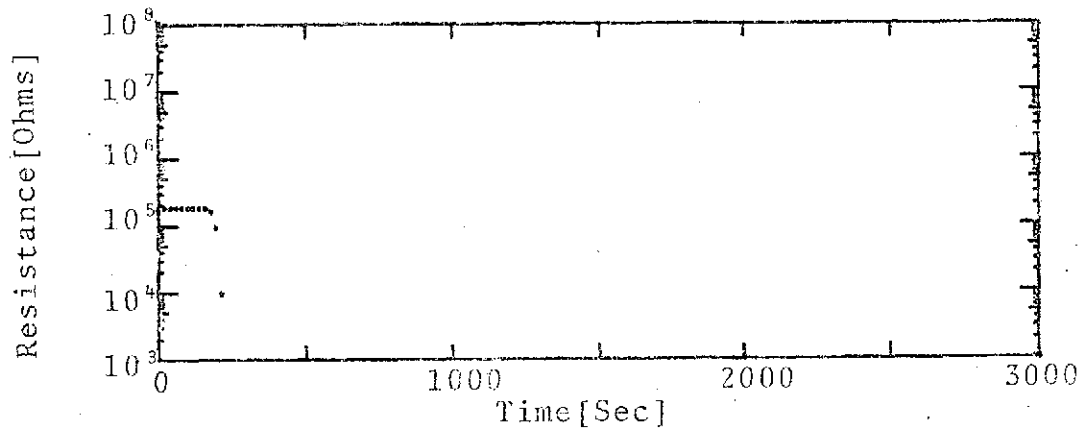
RESULTS

As seen in Fig. 4.10, the D/A voltage started at an initial value of 0.5 volts and remained fixed as the pulse width was varied from 0.0005 seconds to 0.512 seconds. The decay time for each pulse was set at a maximum value determined by the limitations of the D/A converter. At this point the D/A voltage was increased to one volt and the process repeated. An example of the energy variations that occurred due to the applied voltage pulses can be seen from Table 5.1. The energy values were computed using (4.1) and (4.5) and a fixed resistance of 100 k Ω . A sharp drop in energy is noted when the amplifier voltage is increased and the pulse width is reset to 0.0005 seconds. This observation will be useful in explaining the results.

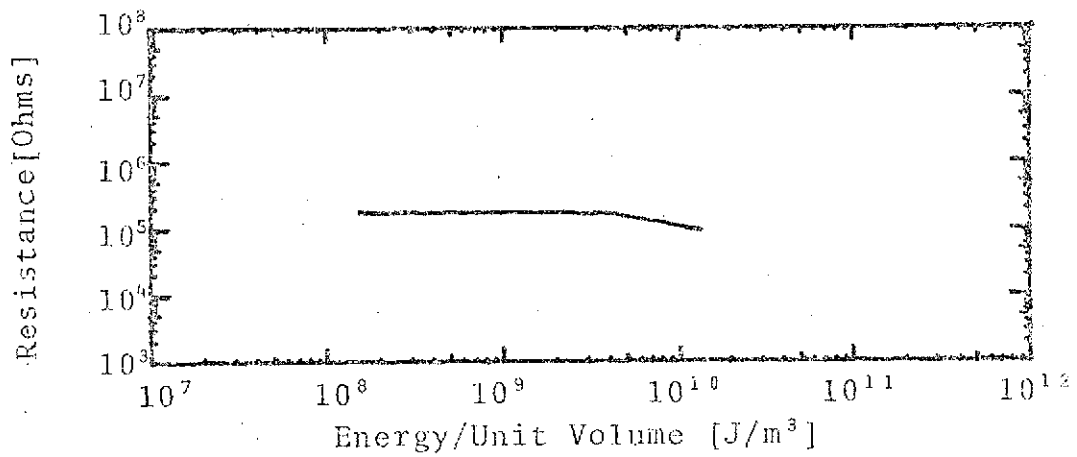
Figures 5.1 through 5.12 show plots of resistance versus time, percentage decrease in resistance versus energy per unit volume, and resistance versus energy per unit volume for each of the devices listed in Table 4.2 which exhibited switching characteristics. The curves shown in part (a) of these figures are the resistance versus time characteristics that were obtained experimentally during the test procedures. The general shape of these characteristics can be explained by looking at the resistance versus energy per unit volume

Table 5.1. Energy of Switching Pulses

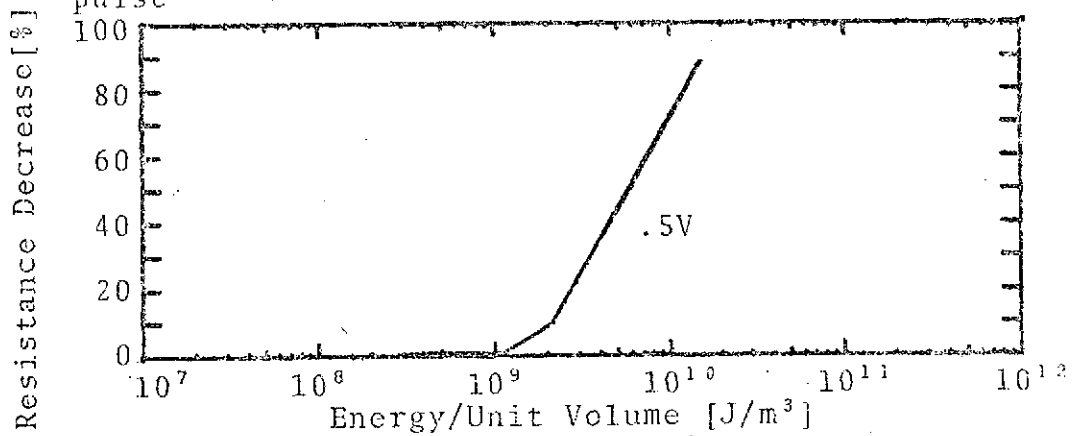
Pulse Height (Volts)	Pulse Width (Seconds)	Decay Time (Seconds)	Energy (Joules) 10^{-6}
13.85	.0005	.02	20
13.85	.001	.02	21.1
13.85	.002	.02	23.0
13.85	.004	.02	26.9
13.85	.008	.02	34.5
13.85	.016	.02	49.9
13.85	.032	.02	80.6
13.85	.064	.02	141.9
13.85	.128	.02	264.7
13.85	.256	.02	510.2
13.85	.512	.02	1001.3
27.7	.0005	.02	80.6
27.7	.001	.02	84.4
27.7	.002	.02	92.1
27.7	.004	.02	107.4
27.7	.008	.02	138.1
27.7	.016	.02	199.5
27.7	.032	.04	399.0
27.7	.064	.04	644.5
27.7	.128	.04	1135.6
27.7	.256	.04	2117.7
27.7	.512	.04	4082.0



(a) Resistance variation during testing

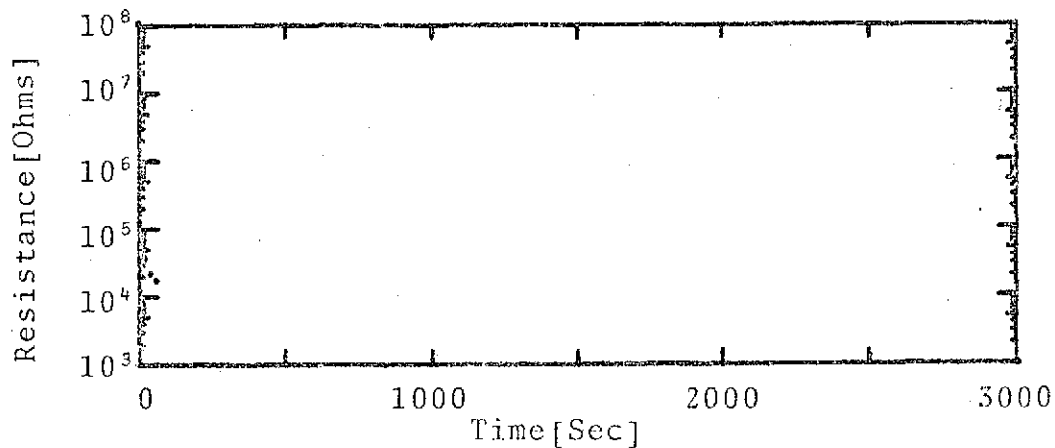


(b) Resistance variation vs. energy density of switching pulse

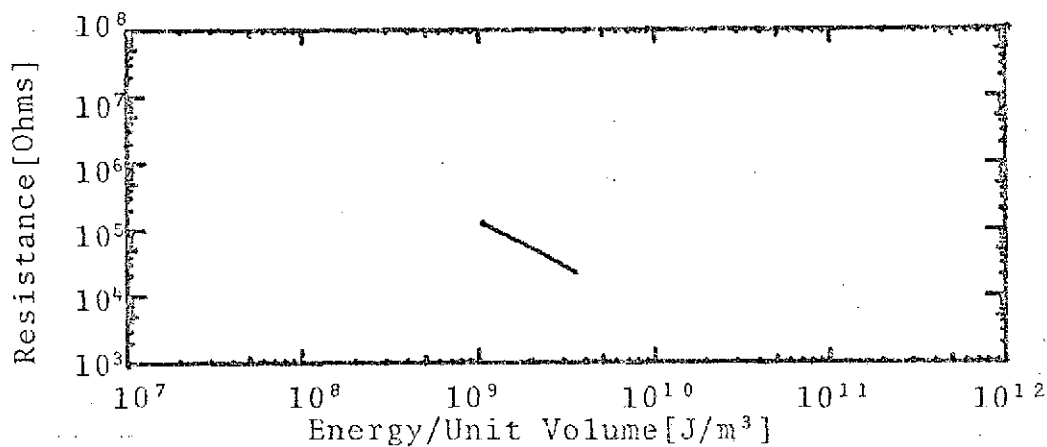


(c) Percentage decrease in resistance vs. energy density of switching pulse

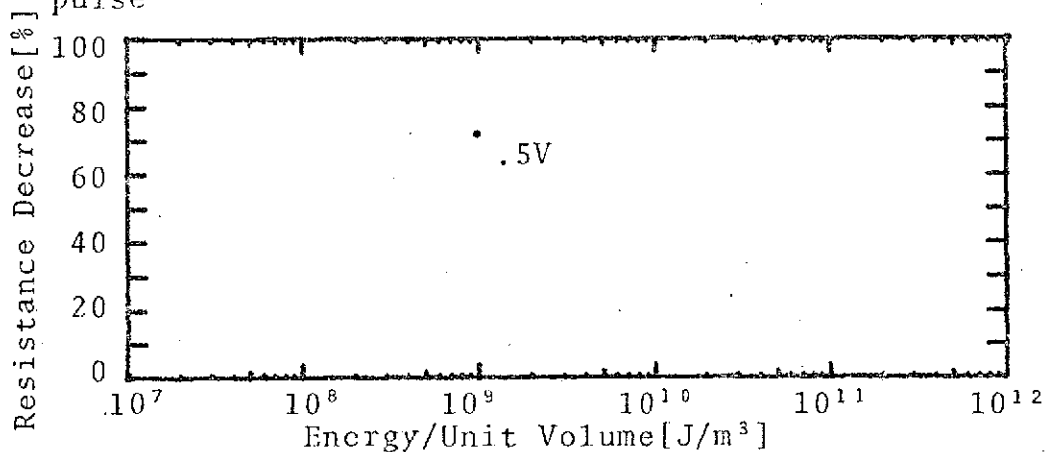
Figure 5.1. Switching Characteristics of Sample A3



(a) Resistance variation during testing

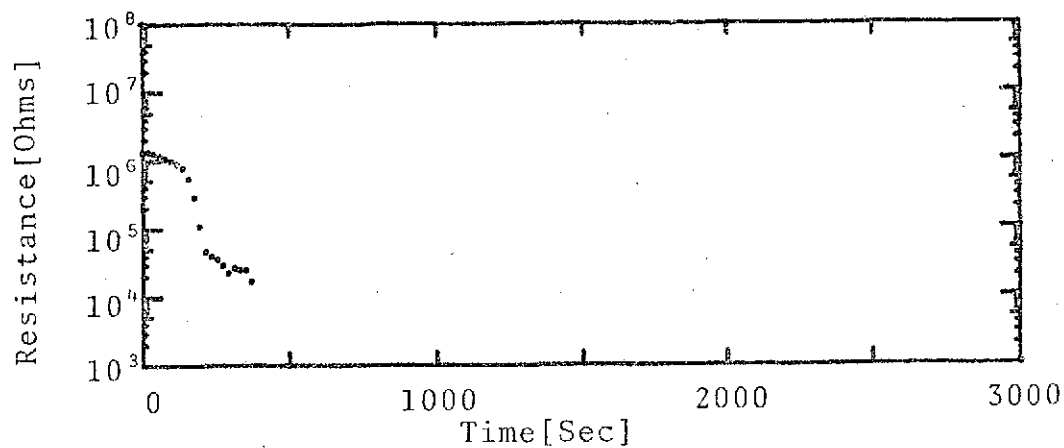


(b) Resistance variation vs. energy density of switching pulse

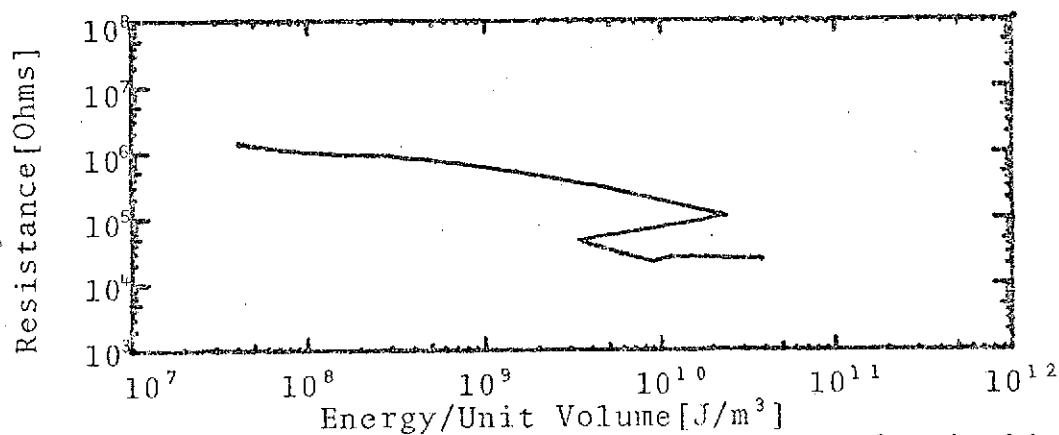


(c) Percentage decrease in resistance vs. energy density of switching pulse

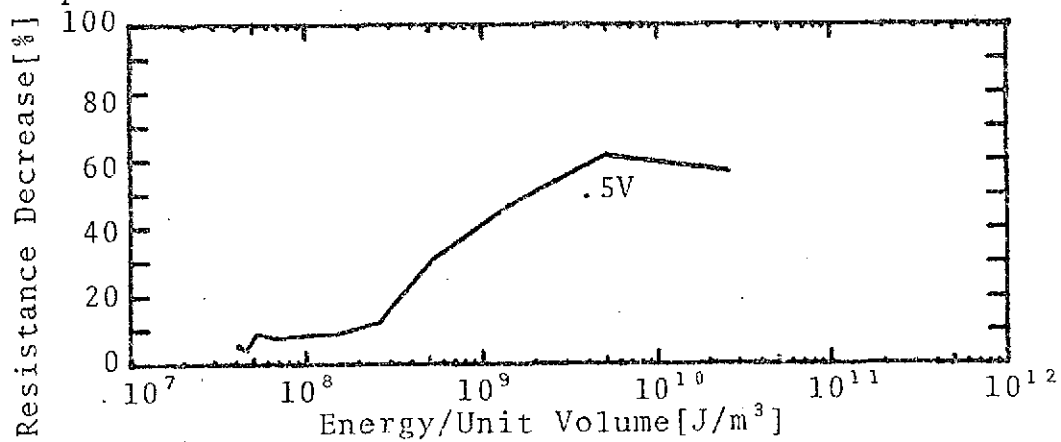
Figure 5.2. Switching Characteristics of Sample C1



(a) Resistance variation during testing



(b) Resistance variation vs. energy density of switching pulse



(c) Percentage decrease in resistance vs. energy density of switching pulse

Figure 5.3. Switching Characteristics of Sample C2

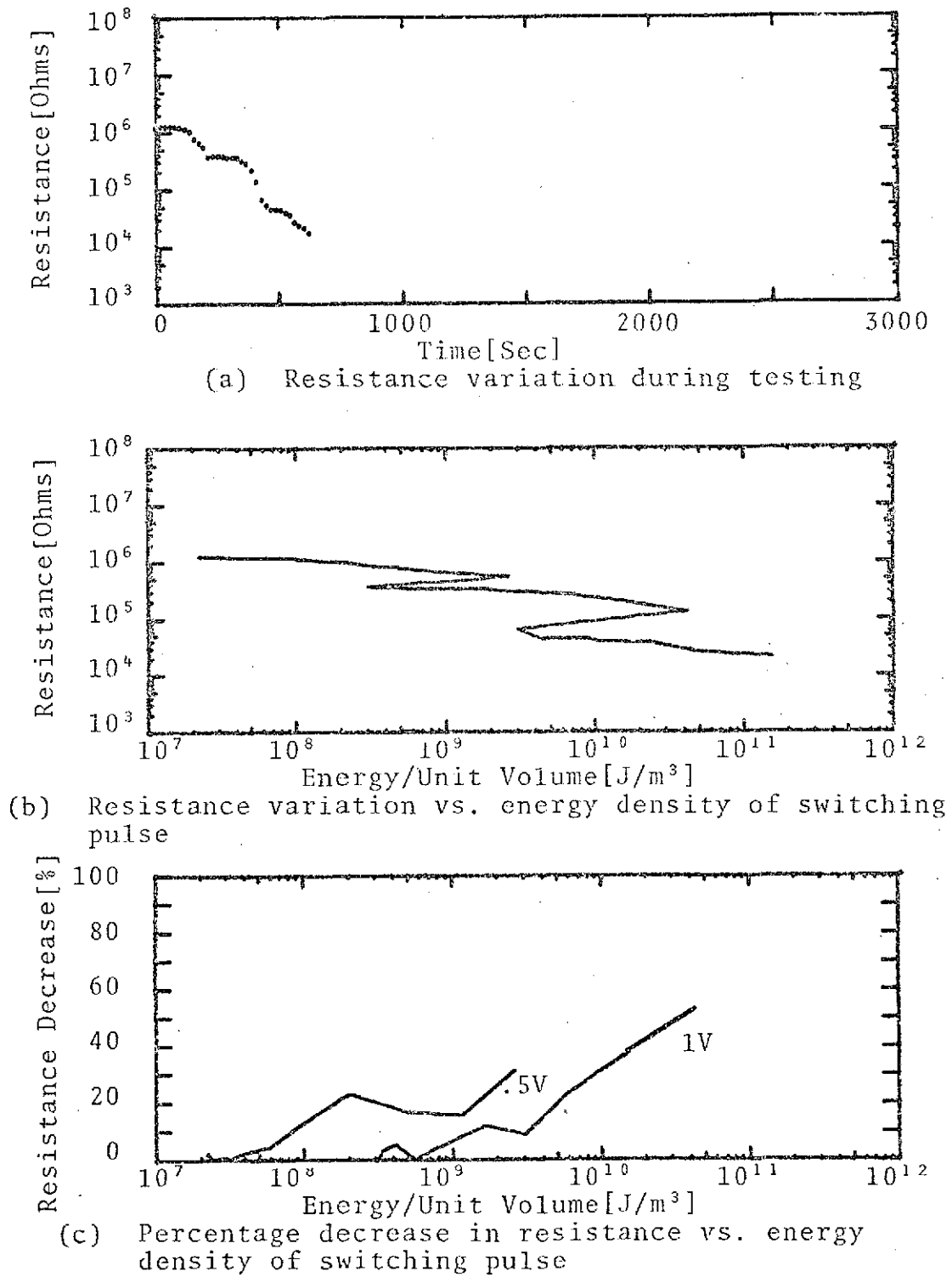
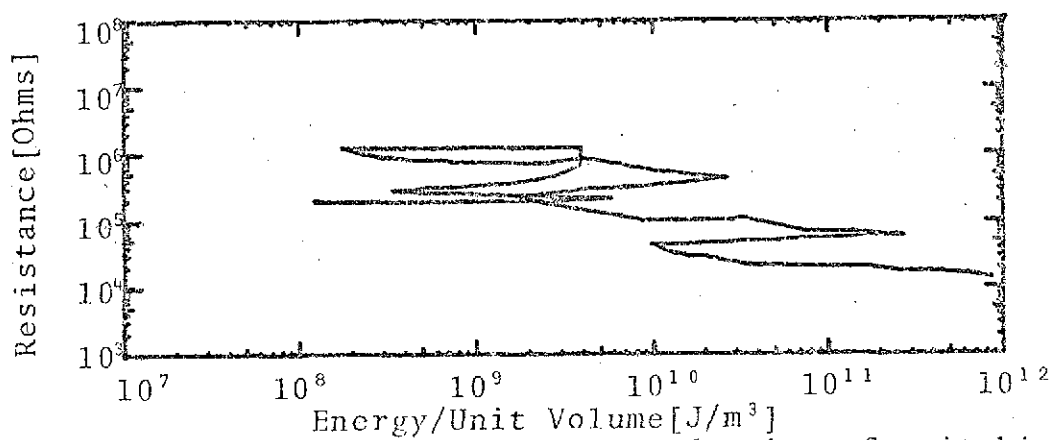
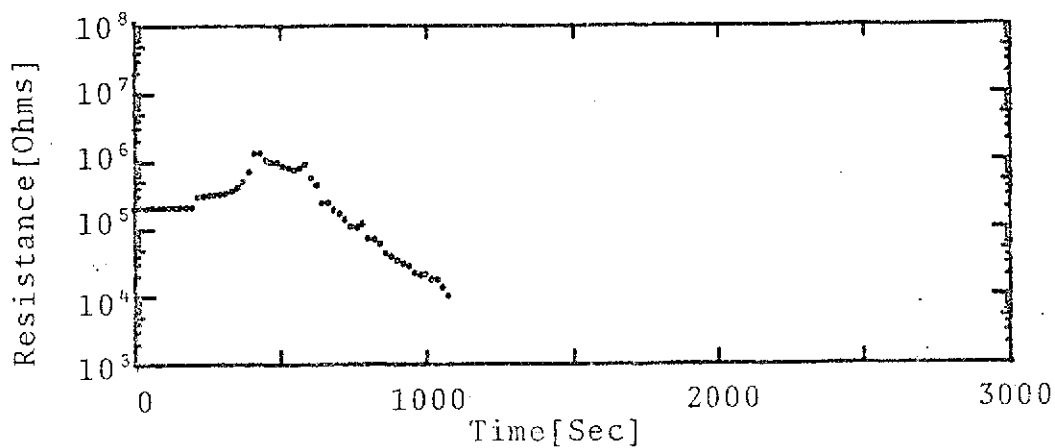


Figure 5.4. Switching Characteristics of Sample C3



(b) Resistance variation vs. energy density of switching pulse

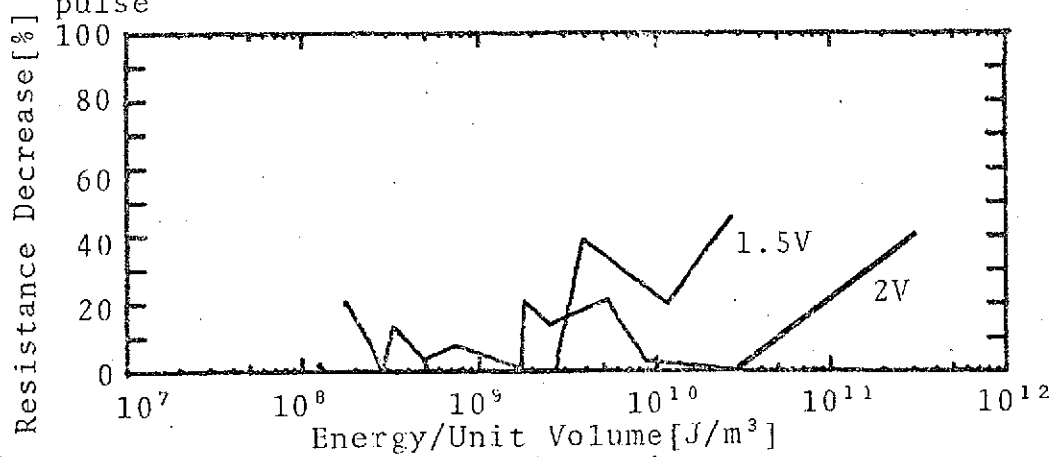


Figure 5.5. Switching Characteristics of Sample D3

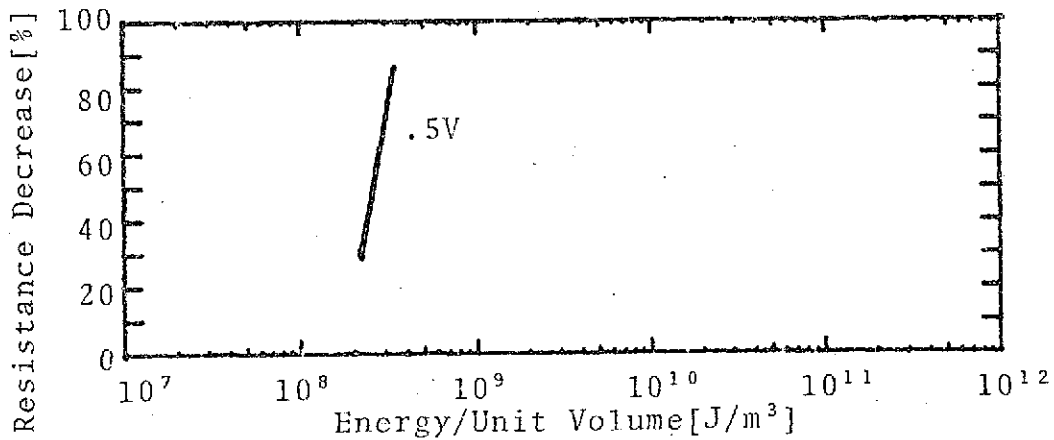
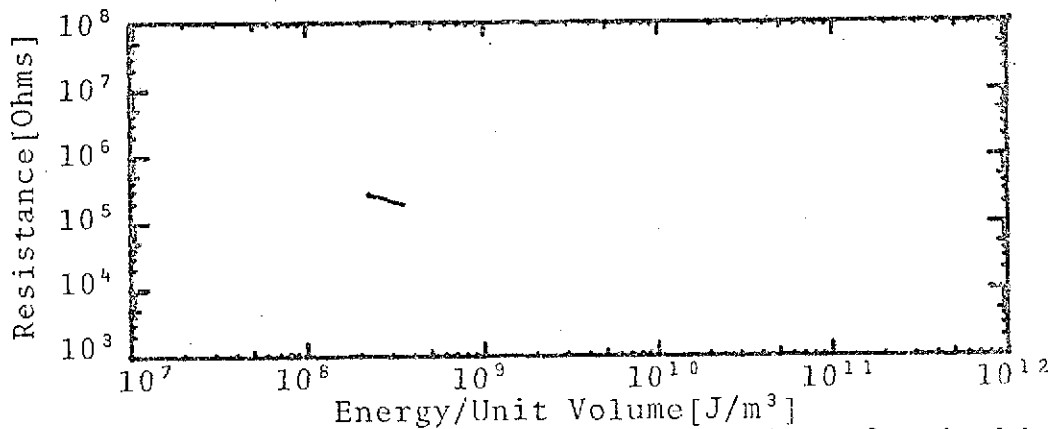
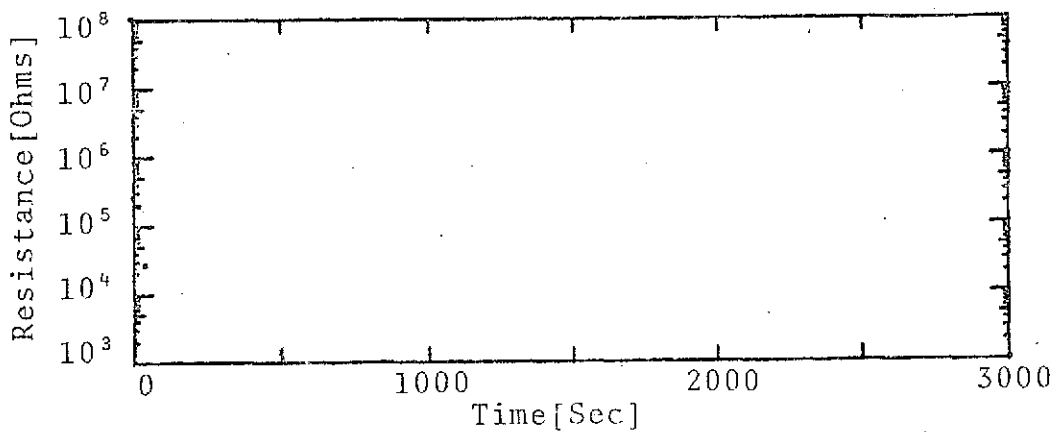
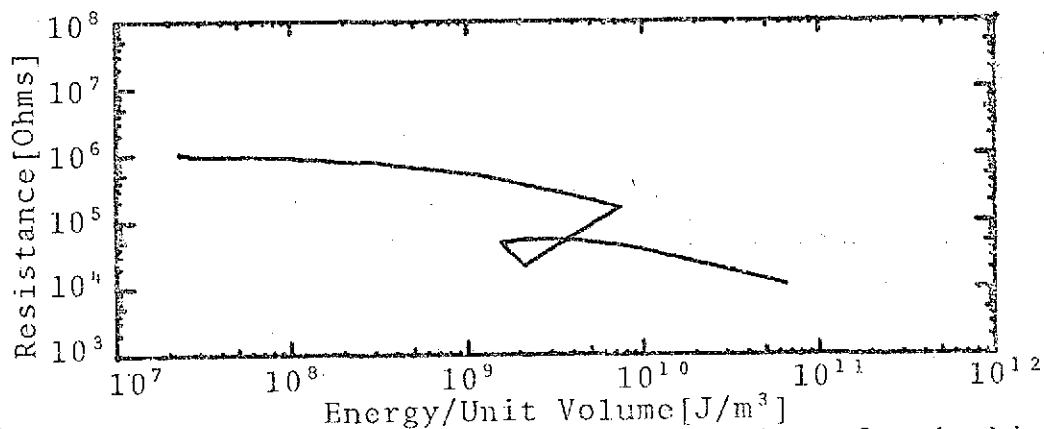
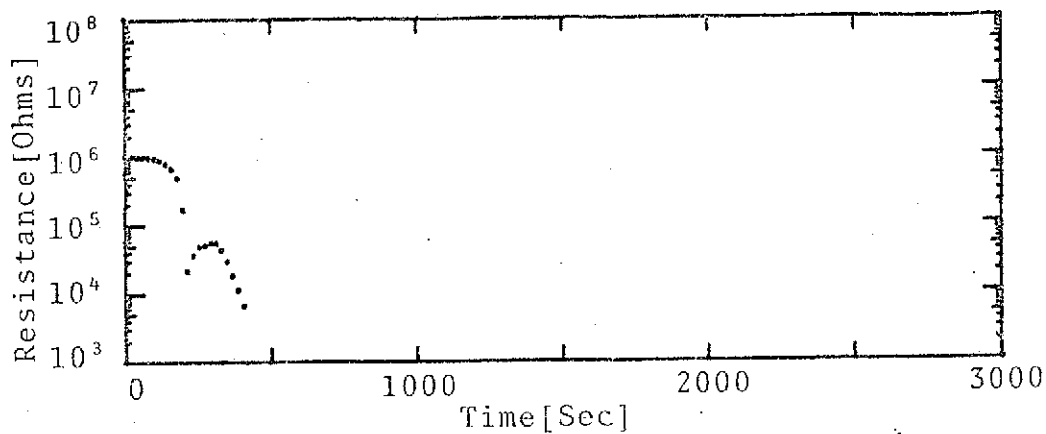
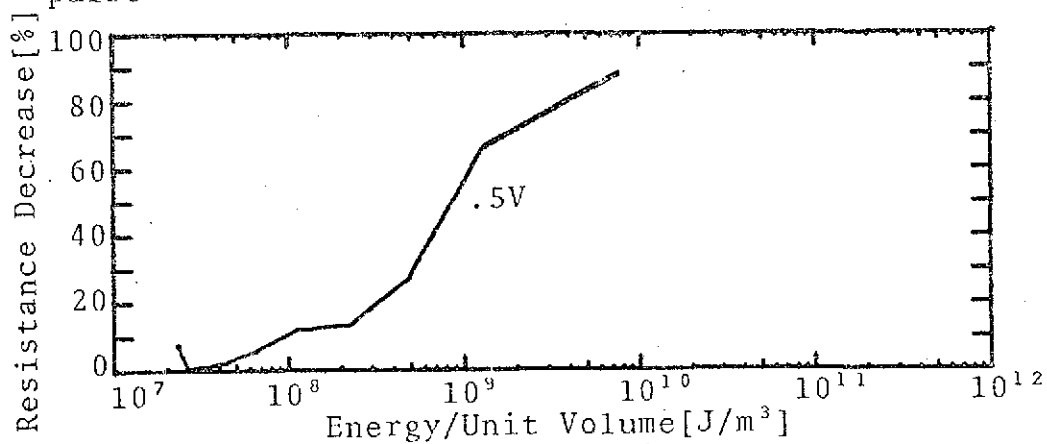


Figure 5.6. Switching Characteristics of Sample E1

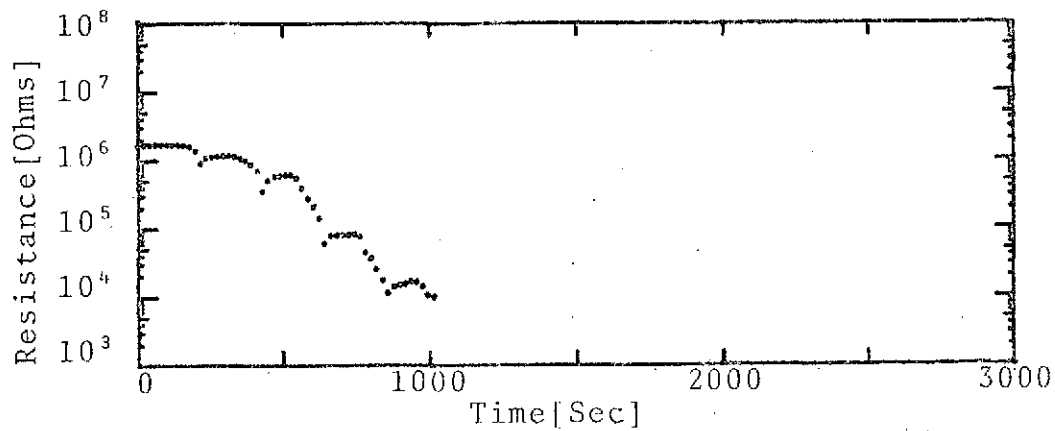


(b) Resistance variation vs. energy density of switching pulse

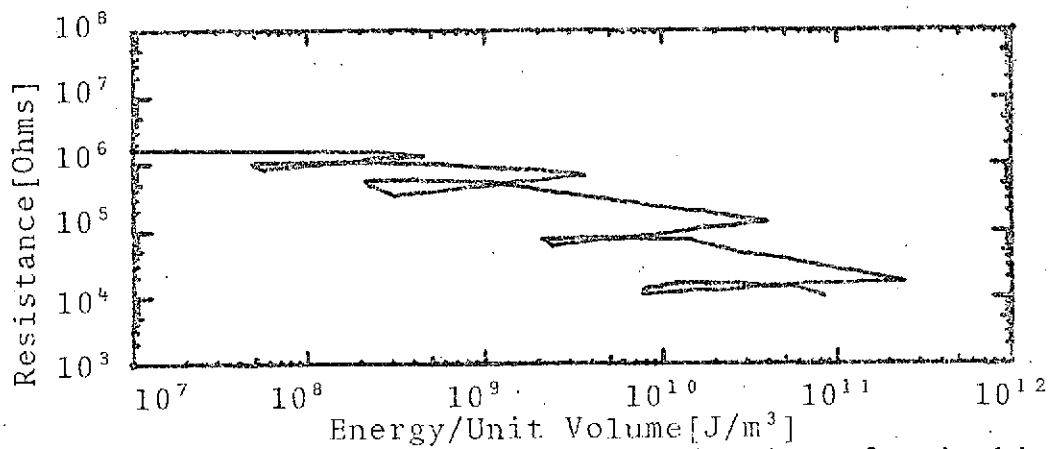


(c) Percentage decrease in resistance vs. energy density of switching pulse

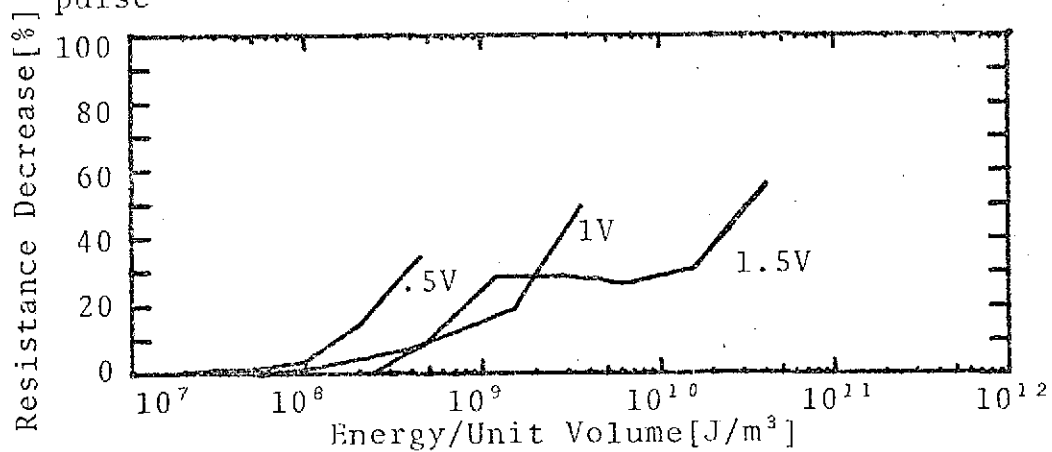
Figure 5.7. Switching Characteristics of Sample E2



(a) Resistance variation during testing

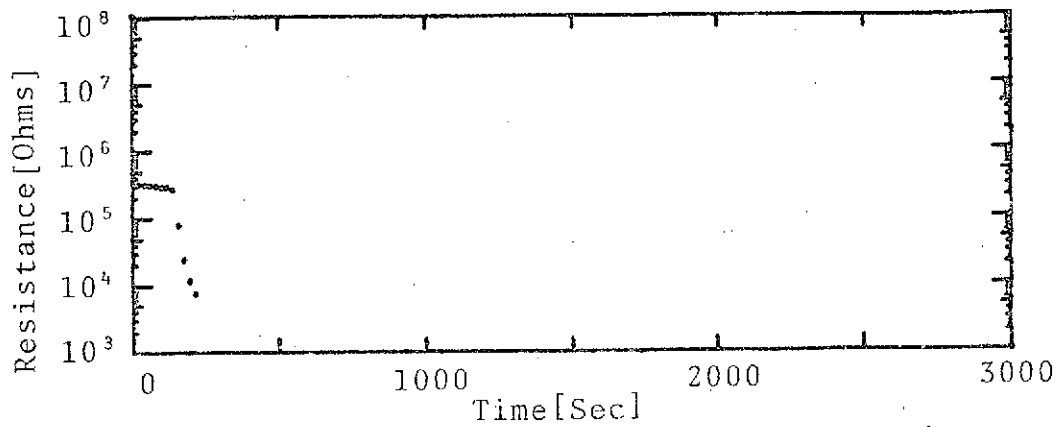


(b) Resistance variation vs. energy density of switching pulse

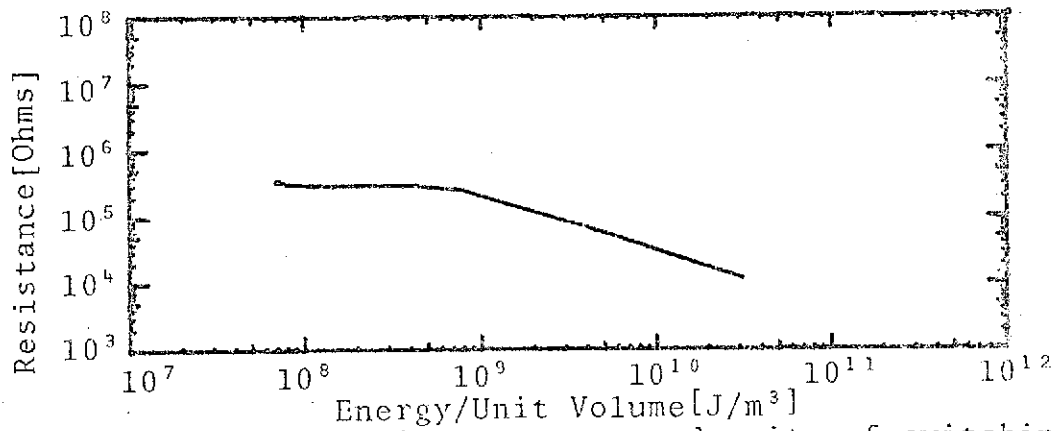


(c) Percentage decrease in resistance vs. energy density of switching pulse

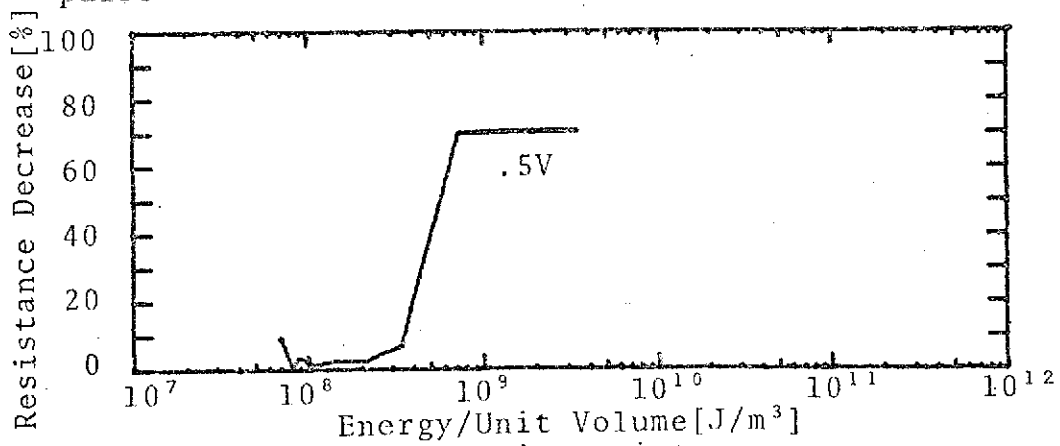
Figure 5.8. Switching Characteristics of Sample E3



(a) Resistance variation during testing

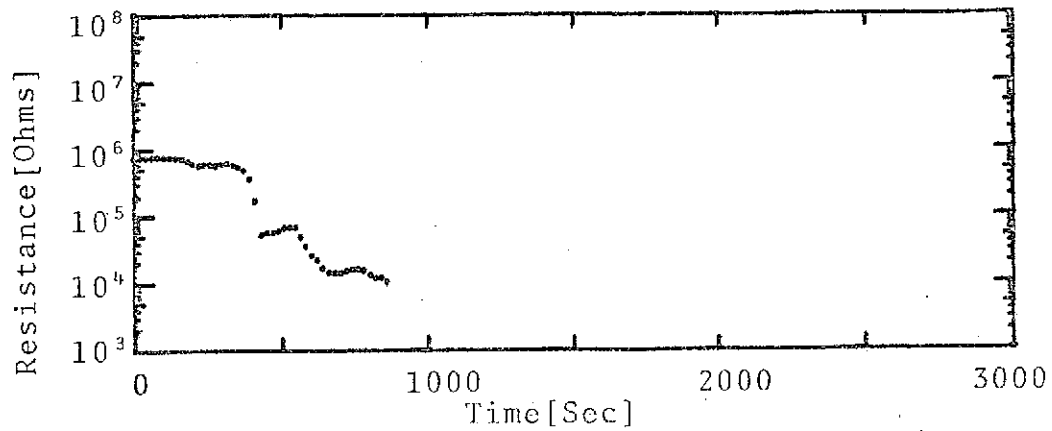


(b) Resistance variation vs. energy density of switching pulse

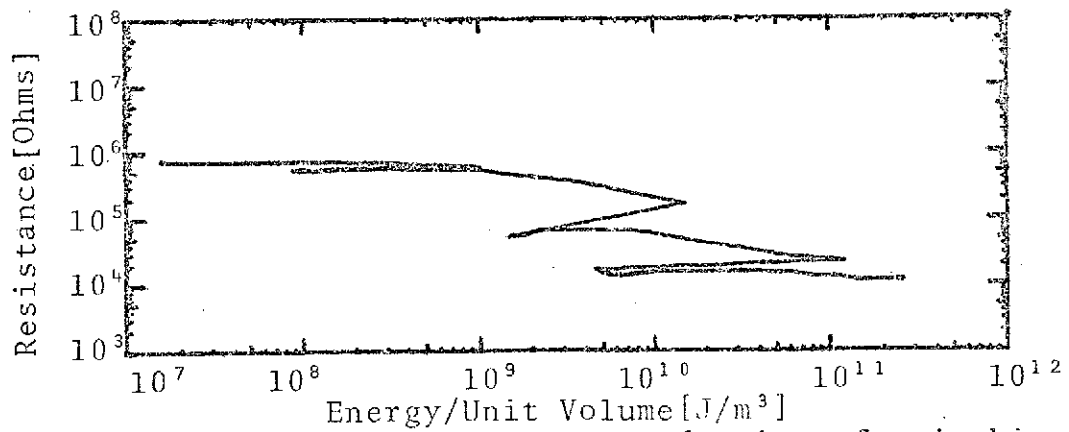


(c) Percentage decrease in resistance vs. energy density of switching pulse

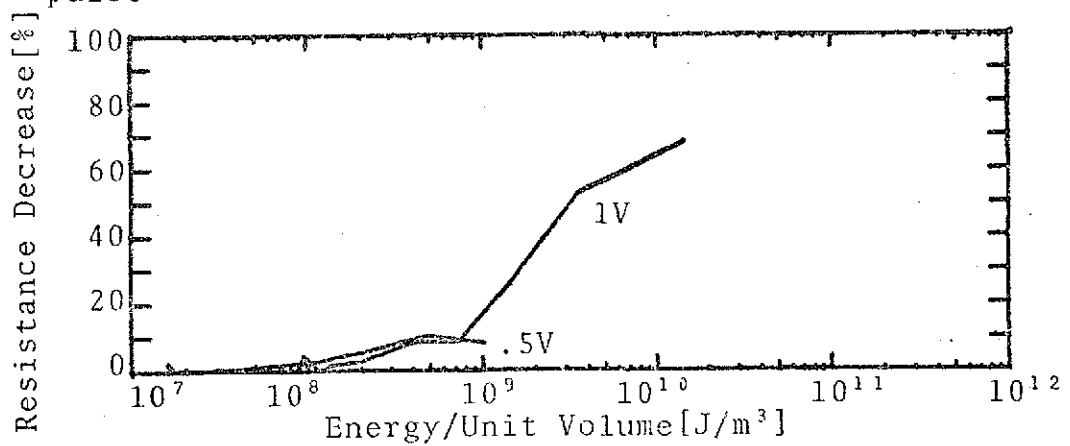
Figure 5.9. Switching Characteristics of Sample F2



(a) Resistance variation during testing

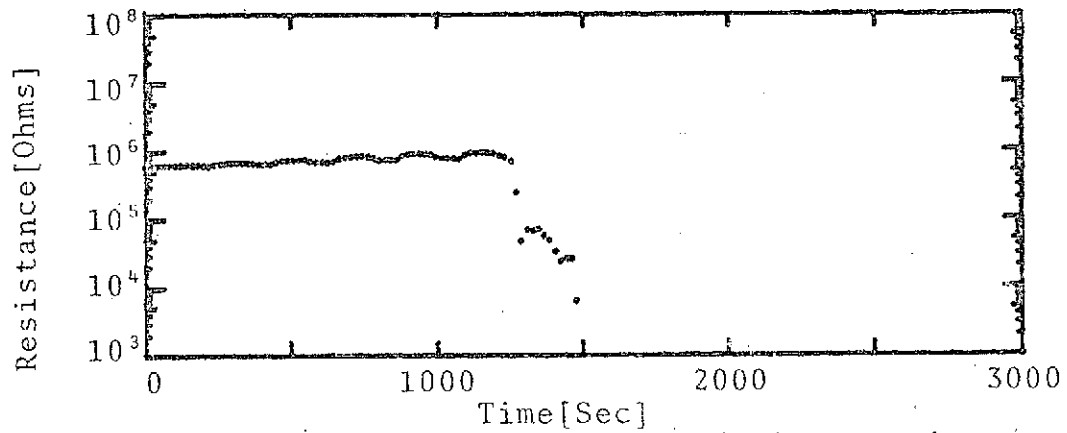


(b) Resistance variation vs. energy density of switching pulse

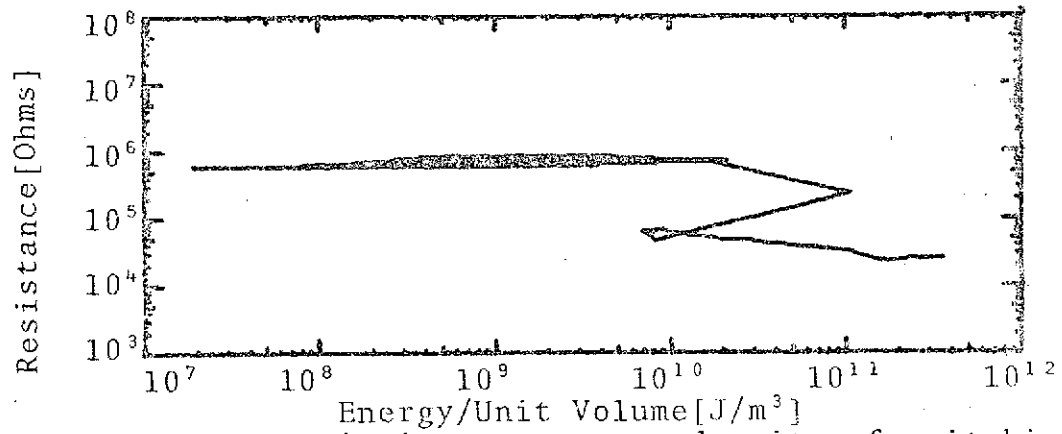


(c) Percentage decrease in resistance vs. energy density of switching pulse

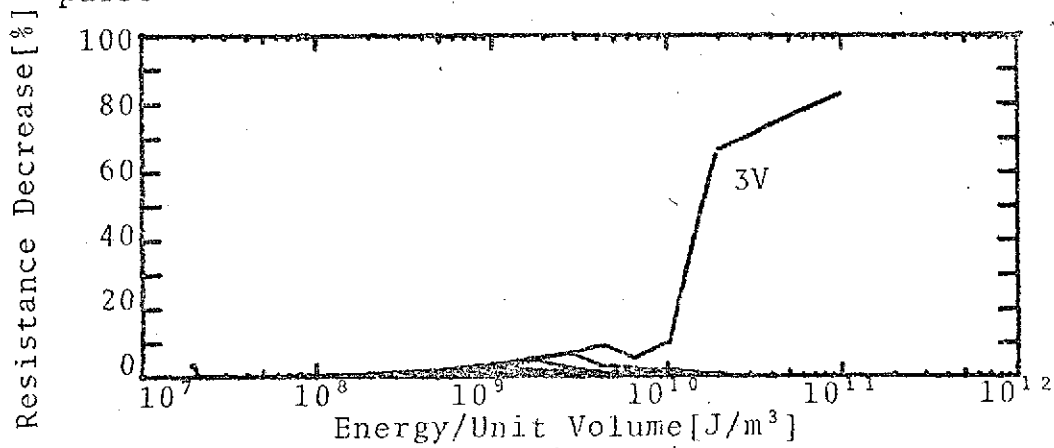
Figure 5.10. Switching Characteristics of Sample F3



(a) Resistance variation during testing

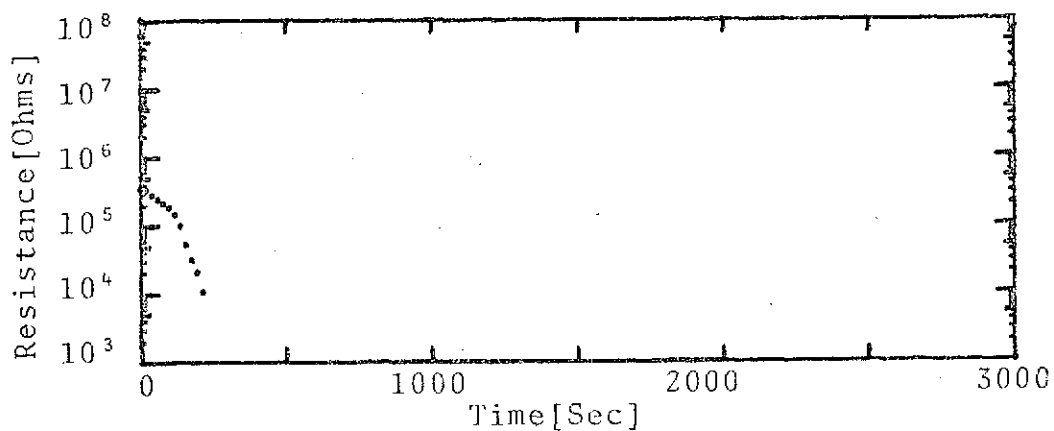


(b) Resistance variation vs. energy density of switching pulse

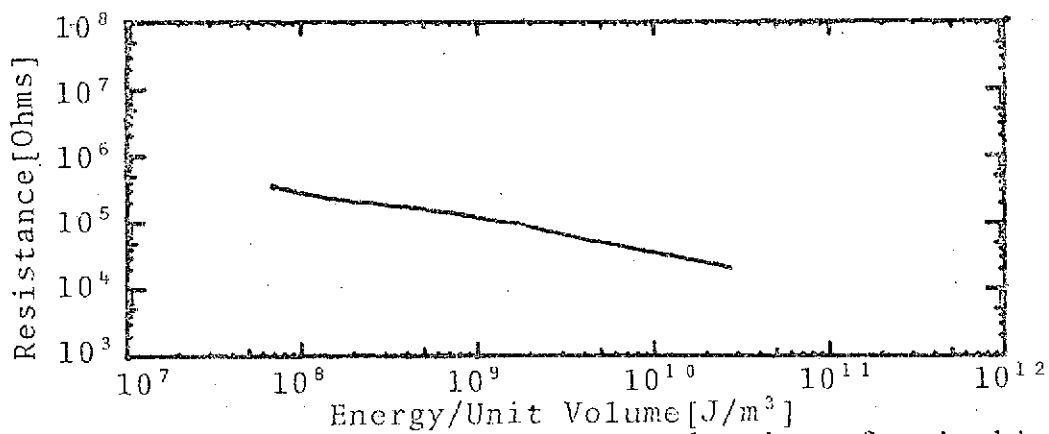


(c) Percentage decrease in resistance vs. energy density of switching pulse

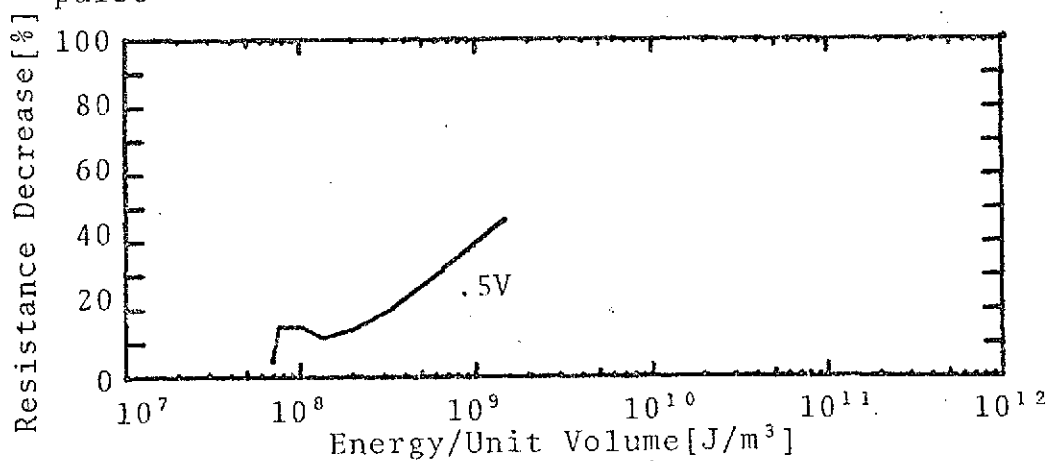
Figure 5.11. Switching Characteristics of Sample G3



(a) Resistance variation during testing



(b) Resistance variation vs. energy density of switching pulse



(c) Percentage decrease in resistance vs. energy density of switching pulse

Figure 5.12. Switching Characteristics of Sample H2

plots in part (b) of the figures and recalling the energy variation of the applied pulses during testing. In general, as long as the energy of the applied pulses continues to increase, the device resistance will decrease. This seems natural since an increase in energy should result in an increase in temperature of the amorphous material, which should result in a decrease in sample resistance. However, when the amplifier voltage is increased and the pulse width is reset to .0005 seconds, there is an accompanying drop in energy, possibly allowing the sample temperature to drop and resulting in an increase in sample resistance. This increase in resistance appears to continue until the energy reaches a value which is consistent with the value it had toward the end of the previous set of pulses. At this time the resistance begins to decrease once again. The resistance versus energy per unit volume plot for sample G3 in Fig. 4.11 indicates that the device resistance started decreasing at an energy value which it had for a previous pulse, but at a higher voltage. This suggests that the resistance changes which occur may possibly be voltage dependent as well as energy dependent. The resistance decrease versus energy per unit volume plots in part (c) of Figures 5.1 through 5.12 show that, in general, the percentage decrease in resistance increases with increasing energy, which is consistent with the explanations given above.

The resistance versus energy per unit volume curves in Figures 5.1 through 5.12 indicate some correlation between

EV

gap width and energy per unit volume. Fig. 5.13 is a bar graph showing the energy density ranges in which maximum changes in resistance were observed for the three gap widths used in this investigation.

The discussion above might lead one to believe that some type of destructive mechanism was responsible for the observed switching due to the amount of energy being supplied to the devices. This is not true in general, however, as it will be shown later that devices can be made to switch back and forth between two distinct resistance states.

As mentioned earlier, the efforts of this study were primarily concerned with taking films that were initially in a high impedance state and determining when and under what conditions they would switch to a low impedance state. Some films that were initially in a low resistance state were able to be switched to a high resistance state, but there was no basis for comparing these results to those already discussed since the switching characteristics depend on the previous history of the sample.

Table 5.2 shows the results of switching a sample back and forth between two distinct resistance states. The sample had a gap width of 2 mils (0.0000508 meters) and a thickness of 1550 \AA and was initially in a low impedance state. The energy-time combinations that resulted in effective setting and resetting of the device are shown in

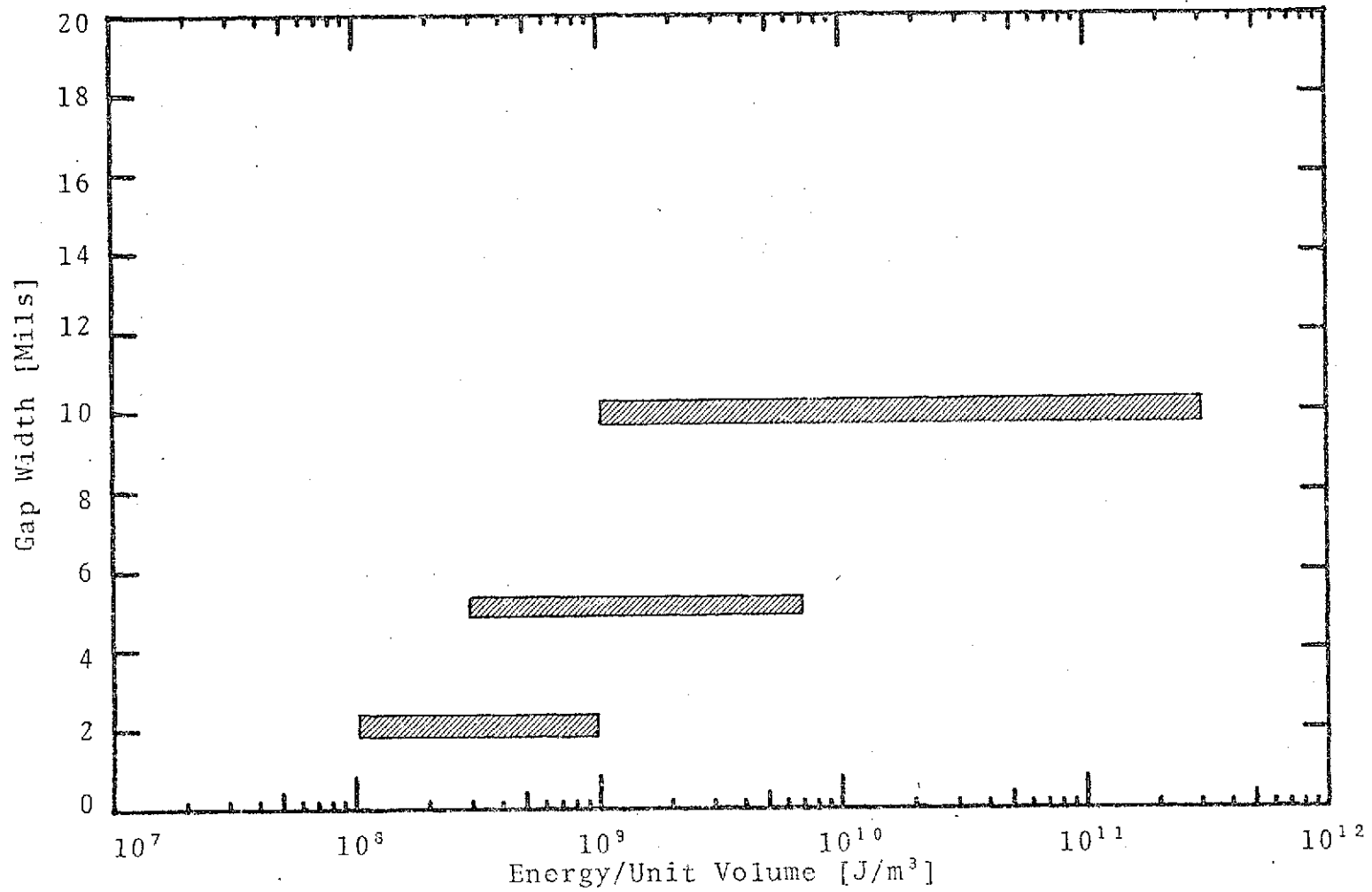


Figure 5.13. Plot of Gap Width Versus Energy/Volume Showing the Range in Which Switching Occurred

Table 5.2. Results Obtained in Switching a Sample
Between Two Stable Resistance States

Sample 4-16-74 1.11
Gap Size 2 mils ($5.08 \times 10^{-5} \text{m}$)
Thickness 1550 Angstroms
Volume $4.0 \times 10^{-14} \text{m}^3$

Resistance Prior to Pulse [Ohms]	D/A Pulse Height [Volts]	Pulse Width [sec] $\times 10^{-4}$	Time Decay [sec] $\times 10^{-5}$	Energy [Joules] $\times 10^{-6}$	Energy/Vol [J/m ³] $\times 10^7$	Resistance After Pulse	Type Pulse
2657.7	.5	5	5	62.6	160	2768.9	U
2768.9	.5	10	5	117.3	293	375204.1	U
375204.1	.5	20	5	1.04	2.59	409151.6	U
485353.5	.5	5	2000	4.1	10.4	489604.1	D
489604.1	.5	10	2000	4.3	10.8	499601.9	D
499601.9	.5	20	2000	4.6	11.5	489724.5	D
489724.5	.5	40	2000	5.5	13.7	486541.4	D
486541.4	.5	80	2000	7.1	17.7	478244.3	D
478244.3	.5	160	2000	10.4	26.1	2977.8	D
3034.9	.5	5	5	55.4	138	522444.5	U

U - denotes switch up pulse
D - denotes switch down pulse

Table 5.2. These results show that SnSe films can be made to switch between two distinct impedance states and that the switching being observed is a nondestructive mechanism.

CHAPTER 6

SUMMARY, CONCLUSIONS AND PROPOSED FUTURE WORK

SUMMARY

The purpose of this research was to determine if Ovonic switching occurred in tin selenide thin films and, if so, what methods could be used to minimize its occurrence. This study was brought about by the observance of inconsistent resistance-temperature characteristics for some of the thin film thermistors being fabricated and tested for NASA. These inconsistencies were attributed to Ovonic switching, although a thorough search of the literature uncovered no record of Ovonic switching having been observed in tin selenide. In all cases, the investigations of Ovonic switching involved the use of bulk amorphous materials or the evaporation of materials which were known to have Ovonic properties. In no cases were the investigations on films under 5000 Å in thickness or of configurations other than sandwich, whereas we were interested in film thicknesses on the order of 1000 Å or less and of a planar configuration.

In order to determine whether Ovonic switching does occur in tin selenide films and under what conditions, a large number of parameters had to be considered. These included the deposition conditions: substrate temperature,

evaporation rate, and film thickness; device geometry: electrode spacing and device configuration; and testing procedures: sample temperature, pulse height, pulse width, and pulse decay time. In addition to the above parameters, the results obtained indicated that source material obtained from different manufacturers could result in samples with quite different characteristics.

During the fabrication process, control was maintained over all the deposition parameters except for deposition rate and source material. There was some difficulty in attempting to control the deposition rate of the tin selenide films. The degree of difficulty seemed to depend on the manufacturer of the material. There were considerable rate fluctuations obtained using the SnSe from one source, whereas the SnSe from a second source could be controlled to within ± 1.5 Hz/sec. during the deposition. Fluctuations such as those observed using the SnSe obtained from the first source could result in a tin rich or selenium rich film which would affect the observed switching characteristics. Another problem to consider is that of contamination of the source material. Since the SnSe used was a fine powder, it is susceptible to trapping impurities and gas particles which could affect the switching characteristics.

To control the parameters associated with the testing procedure, a computer-controlled automatic testing procedure was developed. Based on the published literature, the testing techniques used by other investigators involved the use of a

sinusoidally varying voltage or a square pulse generator with the pulse decay, being controlled by an R-C network. Both of these techniques had very serious drawbacks. The use of an A-C signal meant that only the amplitude of the signal could be controlled, the sample would be continuously heated, and there would be no way to correlate any observed switching properties with either the energy into the sample or the thermal and electronic history of the sample. The use of a square pulse generator for testing of samples was selected initially but proved to be a very slow and tedious process. In addition, the pulse decay time could not be controlled to a high degree of accuracy since the sample itself formed part of the R-C network. For these reasons, an automatic testing procedure was developed which had two major advantages over previously used techniques.

The first advantage was that pulse shape and repetition rate could be adjusted to a wide range of desired values. By using the D/A converter and linear amplifier, pulse heights of greater than 200 volts with a resolution less than 0.1 volt can be obtained. The pulse width can be varied from 0.0001 seconds to 3.2 seconds with a resolution of 100 μ s independent of pulse amplitude. The maximum decay time that can be obtained does, however, depend on the amplitude of the voltage pulse since the smallest increment by which the D/A can be decreased is one bit.

The second advantage of the testing process was the fact that the testing procedure could be programmed on the

computer. This meant that for an hour or more a sequence of pulses of different shapes could be applied to the sample at selected intervals and, based on subsequent measurements, the testing was either continued, terminated, or modified.

The switching properties of the tin selenide films investigated are probably not suitable for use in commercial type devices. Most commercial Qvonic devices use complex compounds such as the chalcogenide glasses to which impurities are added to lower the melting temperature and allow better control of the switching properties. The addition of impurities has also been found to have a marked effect on the lifetime of devices. Since the energy density ranges at which switching occurs in SnSe are now known, it should be possible to fabricate a number of these devices under identical conditions, reduce the voltage variation in the testing procedure, and find an optimum pulse that will result in maximum switching.

There is no adequate theory that presently accounts for the observed switching mechanisms which are taking place. Because of the large variation in parameters in this study, it is hard to isolate electronic and thermal processes. It would not be justifiable to use the data obtained in this study as the basis for a theoretical development to explain Qvonic switching for several reasons. The tin selenide films did not exhibit good switching properties. Rate fluctuations could have caused a wide variation in the composition of the films, leading to different characteristics. The most

feasible approach to developing a mathematical or theoretical model would be to establish switching in an elemental amorphous semiconductor such as germanium or silicon. Once this was accomplished, it would be possible to study the effect of certain types of pulses on the observed characteristics. One approach would be to vary the decay time while holding the pulse height and pulse width constant. This would permit a determination of the effect of decay time on switching properties. Investigations of this nature would help in trying to isolate the mechanisms leading to switching and possibly lead to the formulation of an adequate theory.

CONCLUSIONS

Based on this research, there are several conclusions that can be drawn concerning Ovonic switching in tin selenide thin films. Ovonic memory switching does occur in these films with switching properties being dependent on the energy of the applied pulses. There is also strong implication that the switching is dependent on the magnitude of the applied voltage. The energy densities necessary to observe switching in amorphous tin selenide films are proportional to the spacing between the electrodes of the device (gap width). Although some overlap does exist, the larger gap widths require larger values of energy density for switching to occur. Films with a 2 mil (5.08×10^{-4} m) gap show significant decreases in resistance in the range ($1 \times 10^8 - 1 \times 10^9$)J/m³ while the 5 mil (1.27×10^{-4} m) samples switch in the

(3×10^8 - 7×10^9) J/m^3 range, and the 10 mil ($2.54 \times 10^{-4}m$) samples switch in the (1×10^9 - 3×10^{11}) J/m^3 range. Keeping the values of energy density low will therefore reduce the possibility of switching being observed. This can be accomplished by increasing the volume of the sensing area which means going to a wider gap, a thicker film, or a combination of both. In the work presently being conducted for NASA, it would be possible to increase the film thickness while maintaining the present flight configuration and at the same time reduce the possibility of switching occurring in the films. During this study several films were switched back and forth between two distinct stable resistance states. Since the devices are actually capable of being switched between two states, this implies that the thin film devices are not being destroyed by the high energies and possible high temperatures associated with the applied voltage pulses when switching occurs. That is, the process is reversible.

PROPOSED FUTURE WORK

In order to obtain a better understanding of the switching mechanisms that account for the observed switching phenomena, whether they be electronic or thermal, it is necessary to obtain a large amount of data on films deposited under identical conditions at precisely controlled rates and with a wide variation in gap width and thickness. New mask patterns have already been designed that will allow 21 devices to be deposited on one substrate. Each substrate will contain

seven sets of devices with three devices per set. The gap widths of the seven sets of samples will be 2, 5, 10, 20, 40, 80 and 160 mils. By going to this arrangement, it would be possible to obtain a better correlation between the switching parameters and the deposition parameters.

It has been stated that previous electronic and thermal history could have a marked effect on the observed switching characteristics of a device. This refers to the fact that the observance of the first switching event may require a higher voltage or energy density than subsequent switchings. Once switching has been established, the computer-controlled testing procedure can be programmed to switch the devices back and forth and record the differences in energy densities required to observe switching for subsequent processes.

Based on the results of this study, if a series of pulses are to be used for testing, it is recommended that the pulses be chosen in such fashion that the energy of subsequent pulses is always increasing. This would reduce the fluctuations in resistance caused by possible temperature variations in the material which are a result of applying pulses of varying energy. Another possible variation in testing procedure would be to hold the pulse width fixed and increment the applied voltage.

An investigation of device temperatures during the switching process and their effect on the observed characteristics would provide information which would be useful in

attempting to isolate the thermal and electronic mechanisms of switching. The thin film thermistor being developed for NASA should be capable of detecting temperature changes which occur during switching. By fabricating a structure in which the switching device is deposited over a thin film thermistor, it would be possible to make measurements at different sample temperatures and obtain a great deal of insight into the nature of the switching mechanism.

Scanning electron microscopy studies could also provide useful information in future work and could be used to observe the structure of the material before and after switching had occurred.

The field of Ovonic switching is a relatively new and exciting area and one which holds much promise. However, an extensive expansion in both experimental and theoretical work in the future is needed to further explain the observed phenomena. The suggestions mentioned above would help fulfill this objective.

BIBLIOGRAPHY

BIBLIOGRAPHY

1. Ooten, R. T. "An Investigation of Stability Problems in a Thin-Film Thermistor," Masters Thesis, Tennessee Technological University, August, 1971.
2. Bynum, D. S. "A Study of the Effects of Silver Migration on the Stability of a Thin Film Tin Selenide Thermistor," Masters Thesis, Tennessee Technological University, June, 1972.
3. Palmer, J. L. "The Effects of Substrate Temperature During Deposition and Quartz Encapsulation on the Stability and Response Time of a Thin-Film Tin Selenide Thermistor," Masters Thesis, Tennessee Technological University, June, 1973.
4. National Academy of Sciences. Fundamentals of Amorphous Semiconductors. Washington, D. C.: NAS Printing and Publishing Office, 1972.
5. Henisch, H. K. "Amorphous-Semiconductor Switching," Scientific American, November, 1969, 30-41.
6. Adler, David. "Switching Phenomena in Thin Films," Journal of Vacuum Science and Technology, 10, 5 (September/October, 1973), 728-738.
7. Neale, R. G., D. L. Nelson, and Gordon E. Moore. "Nonvolatile and Reprogrammable, the Read-Mostly Memory Is Here," Electronics, September 28, 1970, 56-72.
8. Ovshinsky, S.R., and H. Fritzsche. "Amorphous Semiconductors for Switching, Memory, and Imaging Applications," IEEE Transactions on Electron Devices, Ed-20, 2 (February, 1973), 91-105.
9. Adler, David, and S. C. Moss. "Amorphous Memories and Bistable Switches," Journal of Vacuum Science and Technology, 9, 4 (July/August, 1972), 1182-90.
10. Ovshinsky, S. R. "Reversible Electrical Switching Phenomena in Disordered Structures," Physical Review Letters, 21, 20 (November 11, 1968), 1450-3.

11. Boer, K. W., and S. R. Ovshinsky. "Electrothermal Initiation of an Electronic Switching Mechanism in Semiconducting Glasses," Journal of Applied Physics, 41, 6 (May, 1970), 2675-81.
12. Fritzsche, H., and S. R. Ovshinsky. "Electronic Conduction in Amorphous Semiconductors and the Physics of the Switching Phenomena," Journal of Non-Crystalline Solids, 2 (1970), 393-405.
13. Guntersdorfer, M. "Thermal Effects Connected with Switching in Amorphous Semiconducting Chalcogenide Films," Journal of Applied Physics, 42, 6 (May, 1971), 2566-7.
14. Henisch, H. K., and R. W. Pryor. "On the Mechanism of Ovonic Threshold Switching," Solid State Electronics, September, 1971), 765-74.
15. Weirauch, Donalf F. "Threshold Switching and Thermal Filaments in Amorphous Semiconductors," Applied Physics Letters, 16, 2 (January 15, 1970), 72-73.
16. Baryshev, V. G., E. V. Vereikin, and P. T. Oreshkin. "Switching Phenomena on the Surface of Glassy CdGeAs₂," Soviet Physics-Semiconductors, 5, 1 (July, 1971), 63-5.
17. Stocker, H. J. "Phenomenology of Switching and Memory Effects in Semiconducting Chalcogenide Glasses," Journal of Non-Crystalline Solids, 2 (1970), 371-81.
18. Warren, A. C. "Reversible Thermal Breakdown as a Switching Mechanism in Chalcogenide Glasses," IEEE Transactions on Electron Devices, Ed-20, 2 (February, 1973), 123-31.
19. Owen, A. E., and J. M. Robertson. "Electronic Conduction and Switching in Chalcogenide Glasses," IEEE Transactions on Electron Devices, Ed-20, 2 (February, 1973), 105-22.
20. Harrison, Walter A. Solid State Theory. New York: McGraw-Hill, Inc., 1970.
21. Yen, J. C. "The Effects of Particle Ionization on the Electrical Properties of Vacuum Deposited Lead Telluride Films," Masters Thesis, Tennessee Technological University, January, 1970.
22. Baxter, C. R. "The Use of Thin-Film Copper-Constantan Thermocouples for Temperature Sensing," Masters Thesis, Tennessee Technological University, August, 1971.